

# A comprehensive review on thermal management systems for power lithium-ion batteries



Wang Zichen<sup>a,b,c</sup>, Du Changqing<sup>a,b,\*</sup>

<sup>a</sup> Hubei Key Laboratory of Advanced Technology for Automotive Components, Wuhan University of Technology, Wuhan, 430070, China

<sup>b</sup> Hubei Research Center for New Energy & Intelligent Connected Vehicle, Wuhan University of Technology, Wuhan, 430070, China

<sup>c</sup> College of Career Technology, Hebei Normal University, Shijiazhuang, 050024, Hebei, China

## ARTICLE INFO

### Keywords:

Thermal management  
Heat pipe  
Phase change  
Heat transfer  
Cooling  
Preheating

## ABSTRACT

Lithium-ion batteries are extensively utilized in electric vehicles for its high energy density. However, safety problems caused by thermal runaway and performance degradation caused by abnormal temperature must be solved. Electric vehicles must adapt to hot and cold environments, which requires the battery pack to keep good performance at both low and high temperatures. A lot of investigations were reported in the last decade on the thermal management techniques of power batteries. To clarify the problems to be solved in the future, the research progress of battery cooling system and preheating system are thoroughly summarized and classified depending on the heat transfer media. Various thermal management technologies are evaluated from multiple perspectives, including production and maintenance costs, system simplification, heating or cooling efficiency, internal temperature gradients, safety, and adaptability. It will be a research trend to design a novel thermal management system incorporating multiple technologies by utilizing the advantages of various cooling and heating methods.

## 1. Introduction

Electric vehicles (EVs) have developed rapidly in recent years to reduce the air pollution. Most EVs choose lithium-ion batteries by reason of high specific energy, good charge retention capacity and no memory effect. Whereas, some problems still restrict its development, such as spontaneous combustion and explode caused by thermal runaway [1–5]. Heat accumulation and local overheating during charging and discharging of batteries are the main causes of thermal runaway [6,7]. Pesaran et al. suggested for lithium-ion batteries that the optimal operating temperature range is 15 °C–35 °C, and the maximum temperature difference in battery modules should remain below 5 °C to avoid negative impacts [8]. The electrochemical reaction in lithium battery is accompanied by exothermic phenomenon and temperature change. The accumulation of heat causes the battery to heat up, which negatively impacts the battery's life, safety, and performance [9–11]. Battery aging is mainly manifested in capacity fading and power loss. The capacity fading is caused by the conversion of active substances inside battery into inactive phases, and power loss is caused by the growing of internal resistance [12–15].

In addition to performance degradation, thermal runaway is another

serious problem caused by overheated batteries is thermal runaway, which means that with the accumulation of heat, the battery may produce gas and even explosion, seriously affecting the safety of vehicles and passengers [16–20]. Uneven temperature distribution in battery pack may also trigger thermal runaway [21,22]. The performance decline of any cell will affect the overall battery pack, and the thermal runaway happened to any cell will lead to battery pack failure [23]. As people demand more mileage for EVs, higher energy density and more cells are needed, so that the heat production and heat accumulation rate of battery pack will be increase. Therefore, an economical and effective battery thermal management system (BTMS) must be adopted to control the temperature in a proper range and maintain the temperature uniformity between batteries.

To insure the battery stability, the researches on BTMS always focus on the cooling of the batteries, but pay less attention to the preheating. Many scholars have reviewed the thermal management technology and aging mechanism of batteries from different perspectives, many of which focused on controlling the temperature rise and preventing thermal runaway in high-temperature environment, while few reviewed the thermal management technology covering the full temperature range [23–30]. This paper divides BTMS into two types according to the ambient temperature: cooling and preheating. The cooling system is

\* Corresponding author. Hubei Key Laboratory of Advanced Technology for Automotive Components, Wuhan University of Technology, Wuhan, 430070, China.  
E-mail address: cq\_du@whut.edu.cn (D. Changqing).

**Abbreviations**

EV	Electric vehicle
BTMS	Battery thermal management system
PCM	Phase change material
1D	One-dimensional
2D	Two-dimensional
3D	Three-dimensional
LP	Lumped parameter
ROM	Reduced-order model
CPCM	Composite phase change material
EG	Expanded graphite
DSC	Differential scanning calorimetry
XRD	X-Ray diffraction
CF	Copper foam
LDPE	Low-density polyethylene
NF	Nickel foam
PEG1000	Poly Ethylene Glycol 1000
Al-foam	Aluminum foam
HP	Heat pipe
HPCD	Heat pipe cooling device
OHP	Oscillating heat pipe
DC	Direct current
AC	Alternating current
SHLB	Self heating lithium-ion battery
PCS	Phase change slurry
SOC	State of charge
PNGV	Partnership for New Generation of Vehicles

**Nomenclature**

q	Heat generation rate of the battery, W
$q_v$	Volumetric heat generation rate, $\text{W}/\text{m}^3$
I	Current, A
U	Voltage, V
T	Temperature, K
$C_p$	Specific heat capacity, $\text{J}/(\text{kg} \cdot \text{K})$
V	Volume, $\text{m}^3$
t	Time, s
$R_h$	Heat-convection thermal resistance, $\text{K}/\text{W}$
h	Convective heat transfer coefficient, $\text{W}/(\text{m}^2 \cdot \text{K})$
A	Convective heat transfer area, $\text{m}^2$
B	Time constant, s
$v$	Velocity of the electrolyte, $\text{m}/\text{s}$
c	Concentration of lithium ions, $\text{mol}/\text{m}^3$
D	Diffusion coefficient of lithium ions, $\text{m}^2/\text{s}$

r	Radial coordinate, m
$r_s$	Radius of solid active material particle radius, m
$j^{li}$	Local volumetric transfer current density, $\text{A}/\text{m}^3$
$a_s$	Active surface area per electrode unit volume, $\text{m}^2/\text{m}^3$
F	Farady's Constant, F = 96,487 C/mol
$t_+^0$	Transference number of lithium ion
x	coordinate across the thickness of the electrode, m
J	Current density, $\text{A}/\text{m}^2$
R	Universal gas constant, R = 8.3143 J/(mol · K)
$j_0$	Exchange current density, $\text{A}/\text{m}^2$
$E_{eq}$	Equilibrium potential of an electrode
k	Thermal conductivity, $\text{W}/(\text{m} \cdot \text{K})$
H	Latent heat, $\text{kJ}/\text{kg}$

**Greek letters**

$\rho$	Density, $\text{kg}/\text{m}^3$
$\varepsilon$	Volume fraction
$\sigma$	Conductivity of the solid electrode, S/m
$\varphi$	Electrical potential, V
$\delta$	Thickness, m
$\kappa$	Conductivity of electrolyte ionic, S/m
$\kappa_D$	Diffusion conductivity of Electrolyte, A/m
$\alpha$	Charge transfer coefficient
$\eta$	Surface overpotential of an electrode reaction, V
$\nu$	Kinematic viscosity, $\text{m}^2/\text{s}$
$\mu$	Viscosity, $\text{Pa} \cdot \text{s}$

**Subscripts and superscripts**

oc	Open-circuit
o	Operating
h	Heat-convection
i	Initial
amb	Ambient
s	Solid phase
e	Electrolyte
se	Surface electrolyte
eff	Effective
n	Negative electrode
p	Positive electrode
sep	Separator
a	Anodic
c	Cathodic
max	Maximum
m	Melting

classified into four modes on the basis of heat-transfer medium: air cooling, liquid cooling, phase change material (PCM) and heat pipe (HP) applications. The preheating system is classified as internal heating and external heating according to whether the battery is a heat source. An overview of the classifications and research progress of BTMS is presented in the paper. The advantages, limitations and suitable conditions of each system are also discussed in terms of future research possibilities.

## 2. Heat generation mechanism and thermal models of lithium-ion battery

The thermal characteristics of lithium-ion battery are determined by the complex electrochemical reaction and electric-thermal conversion. The heat generation consists of four components: reaction heat, ohmic heat, polarization heat and secondary reaction heat. The secondary reaction heat, such as the decomposition heat of small part of electrode or electrolyte at high temperatures, is generally ignored. Reaction heat

refers to the heat generated by the insertion and deintercalation of lithium ions between positive and negative electrodes, which is related to the entropy change. Polarization is the phenomenon that the actual potential deviates from the equilibrium potential as the current flows through the electrode surface. The polarization heat is affected by the voltage difference between average terminal voltage and open circuit voltage. It is related to battery type, current, ambient temperature, etc. Ohmic heat is irreversible heat associated with current and internal resistance.

Bernardi et al. [31] constructed a simplified heat generation model on account of the internal resistance and entropy increasing reaction principle, as Eq. (1). The first term  $I(U_{oc} - U_o)$  refers to ohmic heat and polarized heat and could be substituted with  $IR_t$ , where  $R_t$  represents the total resistance, including ohmic resistance and polarization resistance. Ohmic resistance is related to material properties and battery geometry. The polarization resistance is related to SOC and depends on the polarization of anode and cathode, whose value is positively correlated

with current density. The latter term is the reversible heat during the entropy change.  $T \frac{dU_{oc}}{dT}$  is the temperature influence coefficient, and relates to the electrochemical reactions.

The thermal models for batteries are divided into one-dimensional (1D) models, two-dimensional (2D) models, three-dimensional (3D) models and lumped parameter (LP) models according to the dimension. The thermal models can be divided into electric-thermal models, electrochemical-thermal models and thermal runaway models based on modeling mechanism. The governing equations are summarized in Table 1. Typical electro-thermal models, such as the equivalent circuit models, reflect the input-output relationship of batteries by constructing circuits composed of electronic components. Rint model, Thevenin model and Partnership for New Generation of Vehicles (PNGV) model are typical equivalent circuit models. Table 2 compared the above thermal models for batteries.

Biot number (Bi) is the ratio of heat-convection resistance to heat-conduction resistance per unit area. Lumped analysis can be performed only if  $Bi < 1$ . Xie et al. [32] regarded the battery as a mass point and assumed that its internal material was homogeneous and isotropic. The specific heat and thermal conductivity were assumed constant. The heat generation rate could also be considered constant at sufficiently

small time steps. The energy balance equation was expressed in Eq. (2), as well as the initial conditions and analytical solutions in Eq. (3)(4).

Lin et al. [33] proposed a LP electro-thermal model for LiFePO<sub>4</sub> cylindrical batteries, which was composed of an equivalent circuit model and a two-state thermal model. The equivalent circuit model was used to obtain the terminal voltage, and the two-state thermal model was utilized to obtain the core temperature and surface temperature. As pictured in Fig. 1, the two models interacted through two-way coupling. The voltage and SOC were calculated through the equivalent circuit model according to the circuit parameter I,  $R_s$ ,  $R_i$ ,  $C_i$ . Heat generation Q was obtained by the difference value ( $V_{OCV} - V_T$ ) and I. The core temperature  $T_c$  and surface temperature  $T_s$  were solved by the two-state thermal model according to Q and  $T_f$ . While the core temperature  $T_c$  was utilized to solve the temperature-related parameters for the electrical model. They verified the reliability of the coupled model by two drive cycle tests with a SOC range of 25%~100%, a temperature range of 5 °C~38 °C and a maximum current rate of 22C. Allafi et al. [34] constructed a novel adaptive lumped parameter thermal model for batteries. The model considered not only hevat convection, but heat radiation, which simulated the heat transfer process more accurately. To manage with the nonlinearity of heat radiation, they also proposed a

**Table 1**

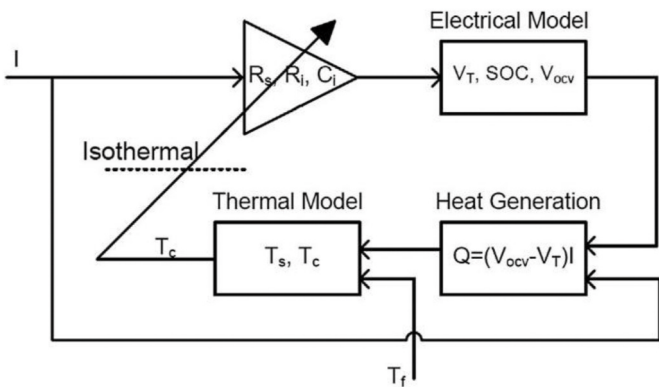
Summary of model equations for batteries.

Types of battery model	Governing equations
Bernardi's heat generation equation	$q = I(U_{oc} - U_o) - I\left(T \frac{dU_{oc}}{dT}\right) \quad (1)$
Lumped thermal model	$\rho C_p V \frac{\partial T}{\partial t} = q - \frac{T - T_{amb}}{R_h} \quad (2)$ $\text{Initial condition: } t=0, T = T_i \quad (3)$ $\text{Analytical solution: } \frac{qR_h - (T - T_{amb})}{qR_h - (T_i - T_{amb})} = \exp\left(-\frac{t}{\rho C_p V R_h}\right) = \exp(-t/B) \quad (4)$
Energy conservation equation	$\rho C_p \left( \frac{\partial T}{\partial t} + v \cdot \nabla T \right) = \nabla \cdot k \nabla T + q_v \quad (5)$
Mass transport equation in the solid phase	$\frac{\partial c_s}{\partial t} = \frac{D_s}{r^2} \frac{\partial}{\partial r} \left( r^2 \frac{\partial c_s}{\partial r} \right) \quad (6)$ $\text{Boundary conditions: } \frac{\partial c_s}{\partial r} \Big _{r=0} = 0; \frac{\partial c_s}{\partial r} \Big _{r=r_s} = \frac{-j^i}{D_s a_s F} \quad (7)$ $\text{Boundary conditions: } \frac{\partial c_e}{\partial x} \Big _{x=0} = 0; \frac{\partial c_e}{\partial x} \Big _{x=L} = 0; \quad (8)$ $\text{Where } L = \delta_n + \delta_{sep} + \delta_p; D_e^{eff} = D_e \epsilon_e^{1.5}; \quad (9)$
Mass transport equation in the electrolyte (1D)	$\epsilon_e \frac{\partial c_e}{\partial t} = D_e^{eff} \frac{\partial^2 c_e}{\partial x^2} + (1 - I_+^0) \frac{j^i}{F} \quad (7)$ $\text{Boundary conditions: } \frac{\partial c_e}{\partial x} \Big _{x=0} = 0; \frac{\partial c_e}{\partial x} \Big _{x=L} = 0; \quad (8)$ $\text{Where } L = \delta_n + \delta_{sep} + \delta_p; D_e^{eff} = D_e \epsilon_e^{1.5}; \quad (9)$
Electrical potential conservation in the solid electrodes (1D)	$\frac{\partial}{\partial x} \left( \sigma^{eff} \frac{\partial \phi_s}{\partial x} \right) - j^i = 0 \quad (8)$ $\text{Boundary conditions: } -\sigma^{eff} \frac{\partial \phi_s}{\partial x} \Big _{x=0} = -\sigma^{eff} \frac{\partial \phi_s}{\partial x} \Big _{x=L} = J; \frac{\partial \phi_s}{\partial x} \Big _{x=\delta_n} = \frac{\partial \phi_s}{\partial x} \Big _{x=\delta_n + \delta_{sep}} = 0; \quad (9)$ $\frac{\partial}{\partial x} \left( \kappa^{eff} \frac{\partial \phi_e}{\partial x} \right) + \frac{\partial}{\partial x} \left( \kappa_D^{eff} \frac{\partial}{\partial x} \ln c_e \right) + j^i = 0 \quad (9)$ $\text{Boundary conditions: } \frac{\partial \phi_e}{\partial x} \Big _{x=0} = \frac{\partial \phi_e}{\partial x} \Big _{x=L} = 0; \quad (10)$
Electrical potential conservation in the electrolyte (1D)	$j^i = a_{ij} j_0 \left[ \exp\left(\frac{\alpha_a F}{RT} \eta\right) - \exp\left(-\frac{\alpha_c F}{RT} \eta\right) \right] \quad (10)$ $\text{Where } j_0 = (c_e)^{a_a} (c_{s,max} - c_{se})^{a_a} (c_{se})^{a_c}; \eta = \phi_s - \phi_e - E_{eq}; \quad (10)$
Butler-Volmer kinetics equations	

**Table 2**

Comparison of thermal models for lithium-ion batteries.

Modeling approach		Characteristics	Computation cost	
Bernardi model	i. Assumes uniform heat generation inside the cell ii. Is based on the entropy increase principle and irreversible heat	i. Requires the overpotential and entropy heat coefficient ii. Ignores the heat convection and radiation heat transfer in the cell	Low	
Electrochemical-thermal model	i. Is based on the First principle ii. Considers the transport of lithium ions and the conservation of charge inside the cell	i. Is able to obtain the current density and potential distribution inside the cell ii. Is more suitable for the simulation of single battery	High	
Equivalent circuit model	Rint model  Thevenin model  PNGV model	i. Assumes that the battery is an ideal voltage source in series with the resistance  i. Is based on the Rint model ii. Connects a parallel Resistance-capacitance network in series  i. Is based on the Thevenin model ii. Adds a capacitor to reflect the accumulation of load current over time	i. Requires fewer parameters ii. Can't reflect the dynamic characteristics of battery charge and discharge iii. Considers no polarization i. Considers the polarization through the resistance and capacitance ii. Is able to simulate the dynamic characteristics of voltage i. Has better dynamic characteristics than the Thevenin model ii. Is more suitable for the simulation of electric vehicles under urban working conditions	Low  Middle  Middle

**Fig. 1.** Two-way coupling between the equivalent circuit model and the two-state thermal model [33].

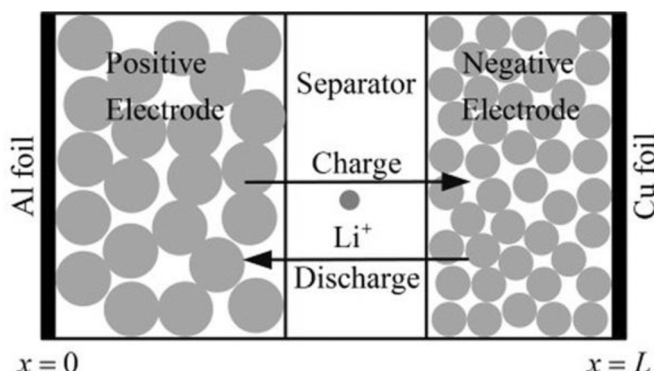
real-time parameter estimation method and verified its effectiveness through experiments. Xie [35] and Richardson et al. [36] investigated algorithms and models for online temperature estimation of battery internal and surface temperature. The improved temperature estimation method considered the internal resistance identification and SOC, which can predict the temperature distribution more accurately.

Wang et al. [37] constructed an electrochemical-thermal coupling model that considered electrode reactions, joule heat, heat conduction, and thermal convection effects to forecast the real-time temperature field inside battery. As shown in Fig. 2, the 1D electrochemical-thermal model consisted of three regions: positive electrode, negative electrodes

and separator. When charged, lithium ions escaped from the positive electrode and embedded in the negative electrode. In the meantime, electrons flowed from the positive to the negative through an external circuit. While during discharging, lithium ions and electrons moved in opposite directions. Lee et al. [38] proposed a 1D discrete-time state-space reduced-order model (ROM) for lithium-ion battery based on physical mechanism. The ROM could predict the electrochemical state accurately at any position on the battery cross-section. The discrete time realization algorithm avoided nonlinear optimization and provided an intuitive method for system-level selection of ROM. The voltage and electrochemical variables predicted by the ROM were consistent with the simulation solution of the fully nonlinear partial differential equations for porous electrodes.

Lithium iron phosphate and lithium manganese oxide are common cathode materials. Tourani et al. [39] constructed a multi-dimensional physical model to investigate their thermal property, which coupled a 1D electrochemical model with a 2D thermoelectric model. The heat generation rate ( $Q_h$ ) and voltage ( $V$ ) under different load cycle conditions were predicted by the 1D model. The surface temperature distribution and current field were obtained by the 2D model. As exhibited in Fig. 3,  $V$  and  $Q_h$  obtained from the 1D model were used as the input terms of the 2D model to solve the temperature and current fields. The weighted average of the surface temperature was then returned to the 1D model and the cycle continued until the results converged. The thermal performance of batteries is affected by the distribution of potential, reaction rate and transport behavior of lithium ions. Xu et al. [40] and An et al. [41] developed 2D electrochemical-thermal models for LiFePO<sub>4</sub> batteries, which coupled electrochemical dynamics and the conservation of mass, charge as well energy. The temperature distribution and electrochemical reaction rate distribution were influenced by heat dissipation conditions and geometric structure. The reaction rate and total heat generation rate of electrodes were obtained and evaluated with natural convection boundary in Ref. [40]. The higher the local reaction rate, the faster the local heat generation rate. During the whole discharge process, the heating in each area of cylindrical battery was relatively uniform, because the position of collector determined the potential distribution, which affected the current and temperature distribution. While the simulated electrochemical reaction rate presented the spatial distribution heterogeneity on the cross-section with the adiabatic boundary, which was determined by the geometric structure [41].

Ghalkhani et al. [42] studied the electrochemical-thermal characteristics such as electric potential, electrolyte phase concentration, and electrode particle heat generation through a 1D multi-physics model. They extended the 1D model to a 3D battery model to investigate the temperature field and current density in a pouch lithium-ion battery. On

**Fig. 2.** 1D electrochemical-thermal model [37].

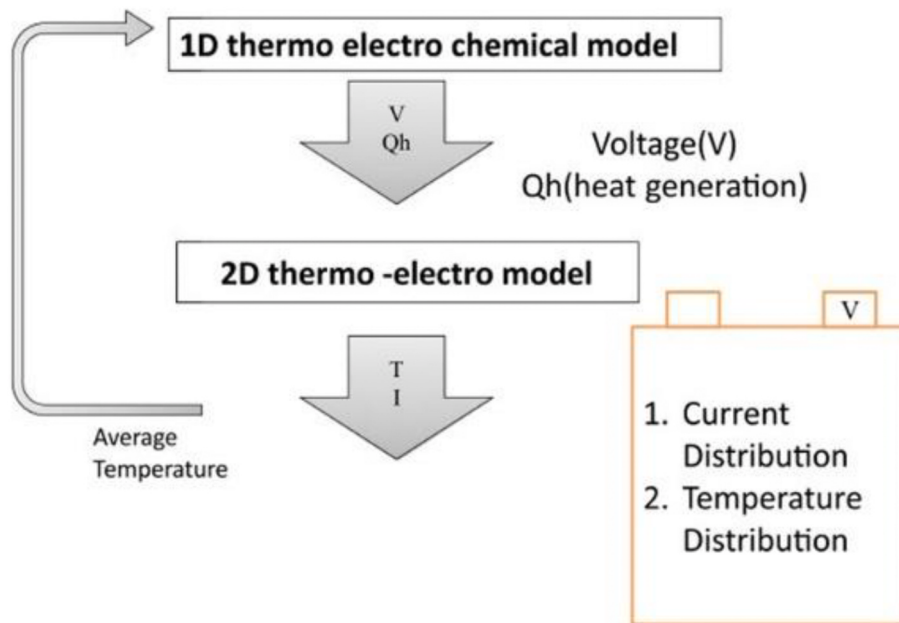


Fig. 3. Sequence of the multi-dimensional model [39].

the grounds of the temperature field curve obtained from the 3D model, the most heat accumulated around the positive electrode of the battery because of the uneven current distribution and local internal resistance. McCleary et al. [43] also constructed a 3D electrochemical-thermal coupled model to simulate thermal characteristics and operation of a LiFePO<sub>4</sub> battery with spirally wound and prismatically wound structures. The interaction between electrochemical properties and temperature distribution was studied by coupling model. Xie et al. [44] believed that the influence of electrode potential distribution and thermal characteristics of tabs on the heat generation distribution could not be ignored. Based on the thermal models of the cell body and tabs, they established a 3D electro-thermal model of the pouch battery. The average static error of the model on the temperature distribution of the battery body is only 0.627 K.

Thermal runaway is one of the causes for battery safety accidents. It is essential to explore the voltage and temperature changes during charging and discharging to ensure the thermal safety. Ren and Feng et al. [45,46] explored the mechanism and thermal characteristics of thermal runaway by establishing an electrochemical thermal coupling model. The voltage and temperature changes during thermal runaway was predicted. They simulated the decay mechanism of battery capacity and analyzed the exothermic chemical reactions at extremely high temperatures. The reliability of the model was proved through comparing the simulated solution with the experimental data [45]. The electrochemical and thermal characteristics under overcharge conditions were also predicted by overcharge-to-thermal-runaway coupled electrochemical-thermal model. The oxidation reaction of electrolyte and the reaction between lithium deposition and electrolyte were the main causes of heat generation in the overcharging process. The modeling analysis of the key parameters proved that the effective way to obtain the better overcharging property of battery was to raise thermal-runaway onset temperature and oxidation potential of the electrolyte.

### 3. Battery cooling systems

#### 3.1. Forced air cooling system

Air cooling systems dissipate heat through direct heat transfer among air and battery, including natural convection and forced convection

[47]. Air natural-convection cooling is extensively applied because of less components and low price, but it cannot meet the requirement of high current discharge [48–50]. Yu et al. [51] experimentally discovered that air natural-convection cooling could keep the maximum temperature and temperature difference in battery pack within ideal range at 0.5C discharge rate. However, the battery pack still needed efficient BTMS for reducing the temperature at high rates of charge and discharge. Forced air-cooling systems are used in Toyota's Prius hybrid and Honda's Insight hybrid [52]. Forced air-cooling systems always rely on fans to drive air circulation and consume extra energy, which is active cooling [51,53]. Forced air cooling has been proved to be able to control temperature rise to a certain extent [54–56]. However, as a result of low specific heat capacity and thermal conductivity of air, the system is not ideal in controlling temperature rise and maintaining temperature uniformity. Compared with the same flow of liquid, the heat dissipation efficiency of air cooling is lower [57]. To enhance heat dissipation, the air-cooling system takes lots of air to cool the cells, resulting in larger piping and valve body sizes and high fan energy consumption. It would limit the application of air-cooling systems in EVs with greater capacity and longer range [58–61].

For the purpose of improving the temperature uniformity and cooling efficiency, many researches focus on optimizing air flow channel and battery pack layout [62]. The design of inlet and outlet also affects the flow field of the battery pack. Yu et al. [63] built a bidirectional flow BTMS to enhance the air-cooling efficiency. The system consisted of two independent inlets and fans, as pictured in Fig. 4. One was to dissipate heat from the batteries by the conventional air ducts, and the other minimized the heat accumulations in the center of battery pack by jet cooling. The numerical results demonstrated that the heat accumulation in the middle cells was greatly decreased through jet cooling and the maximum temperature dropped from 42.3 °C to 33.1 °C. The heat conduction between the baseplate and cells was enhanced by input cooling air in the bottom channel. A 1D coupled thermal-electrochemical model for forced-convection air cooling in battery module was constructed in Ref. [64], indicating that improving the inlet velocity and reducing the cell spacing can reduce the temperature rise. The more homogeneous temperature field was realized through gaining the inlet speed, settling staggered units or increasing the reversing frequency of the periodic airflow. However, it increased the additional load and module volume, so these parameters ought to be

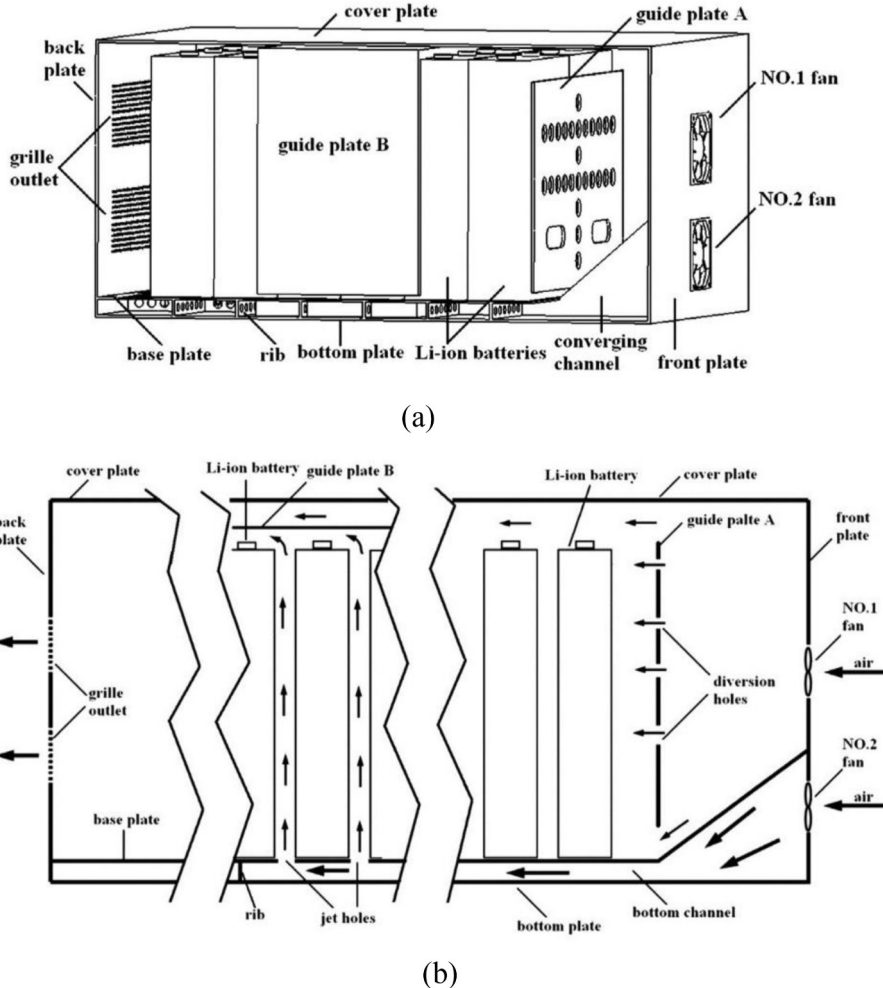


**Fig. 4.** Schematic of the two-directional air flow cooling pack. (a) 3D view. (b) Side elevation [63].

weighed. The cooling effect of the air-based BTMS on the aligned, staggered and intersected battery packs was investigated experimentally, and the conditions of different inlet speeds were compared through experiments in Ref. [65]. The cooling performance and temperature homogeneity of aligned arrangement were the best, staggered and intersected arrangement the next. As the inlet velocity increased, the parasitic power consumption increased exponentially. The aligned arrays have the lowest power consumption, which is 23% lower than cross arrays. In order to obtain the best cooling strategy, E et al. [66] experimentally and numerically compared various cooling strategies by varying the locations of inlet and outlet. Baffles are utilized to change the flow field. The opposite side of inlet and outlet had better cooling effect than the same side, as exhibited in Fig. 5. Xu and He [67] investigated the cooling performance of different airflow strategies and the flow field of the vertically and horizontally arranged battery pack, as Fig. 6 showed. The horizontal layout had shorter airflow path, which enhanced the heat dissipation. Besides, they found that adding bottom duct can increase the heat transfer area and the bottom duct mode with double "U" type had a better cooling performance.

Park Heesung [68] numerically designed and studied air cooling channels for battery packs in hybrid vehicles. The results proved that the use of tapered manifold as well as pressure reducing and ventilation can effectively dissipate heat without changing the arrangement of battery pack. The cooling performance of U-type flow and Z-shaped flow were compared in Ref. [69] (Fig. 7). The simulation results indicated that tapered upper and lower ducts can decrease the flow rate and slow the trend of temperature rise. The lumped battery maximum temperature

was further reduced by inserting corrugated plates with appropriate period length and thickness in the pack. The temperature uniformity depended on the air velocity field in channels, while the flow velocity field was affected by the pressure difference among channels.

Chen et al. carried out a series of studies on air-cooled BTMS. They found that although the maximum temperature could be decreased by improving the inlet velocity, the drive power consumption would raise significantly [70]. They combined the flow resistance network model with the thermal model to propose the structure improvement. The improved BTMS had good cooling effect at different inlet speeds [71, 72]. The feasibility of the flow resistance network model was verified by comparing with CFD method in solving the cooling channel velocity. It was available design the air duct without changing the system volume for optimizing the BTMS. The optimal plenum widths of inlet and outlet were obtained by Newton method and flow resistance network model. On the premise of constant heat generation, Chen et al. also optimized the fixed inlet velocity and fixed power consumption, which reduced the maximum temperature difference by 45% and 41%, respectively [73]. The nest-loop algorithm and simulation were adopted to improve the angles of plenum and size of ducts, thereby raising the efficiency of U-type parallel air-cooled system. The maximum temperature and the temperature difference weren't effectively decreased by setting the angles of the plenums, while optimizing the widths of ducts reduced the temperature difference and the power consumption by 70% and 32% at 5C discharge rate [74]. In addition, Chen et al. [75] numerically researched the effect of inlet and outlet location on heat dissipation. The symmetrical thermal management system with inlet and outlet located

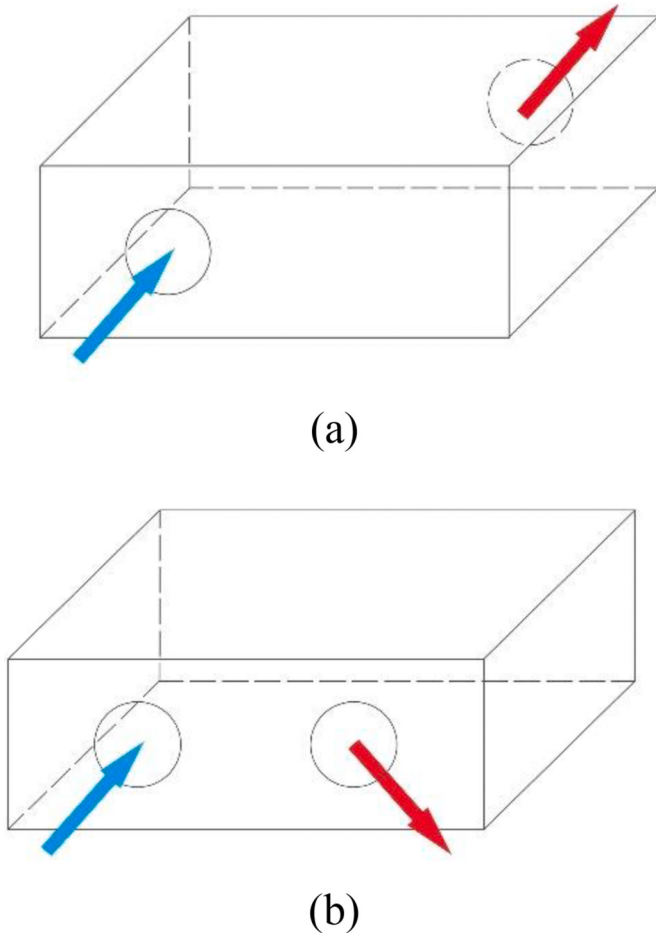


**Fig. 5.** Lateral inlet and outlet. (a) Inlet and outlet located on the opposite side. (b) Inlet and outlet located on the same side [66].

at the middle of plenums had a higher cooling efficiency.

The effect of inlet and outlet angles and the duct width on cooling cells were investigated through experiments and simulation in Ref. [76]. These structural parameters were optimized by orthogonal test and single factor analysis. The thermal performance was best when the inlet and outlet angles were both  $2.5^\circ$  and the duct widths were the same. After multi-objective optimization, the maximum temperature and temperature difference were decreased by 12.82% and 29.72%. The cooling performance of parallel air-cooling system was enhanced by the secondary vent in Ref. [77]. On the condition of constant heat generation rate, the maximum temperature with the secondary vent near outlet was at least 5 K lower than the non-secondary vent system, and the temperature difference was at least 60% lower. Cell spacing is also a parameter that affects the temperature characteristics. Through the 3D transient analysis, Fan et al. [78] demonstrated that the maximum temperature was decreased through reducing the cell spacing or increasing the flowrate of fan, while an optimal temperature uniformity needed a moderate spacing. In addition, Park et al. [79] demonstrated a small-spacing broad battery pack was suitable for air cooling BTMS. Although the optimized design of airflow and battery layout can enhance the heat dissipation to a certain extent, air cooling is not suitable for extreme high-current discharge conditions for its low thermal conductivity and specific heat capacity.

### 3.2. Liquid cooling system

The application of air-cooling system in high power EVs is limited. As listed in Table 3, the thermal conductivity and specific heat capacity of

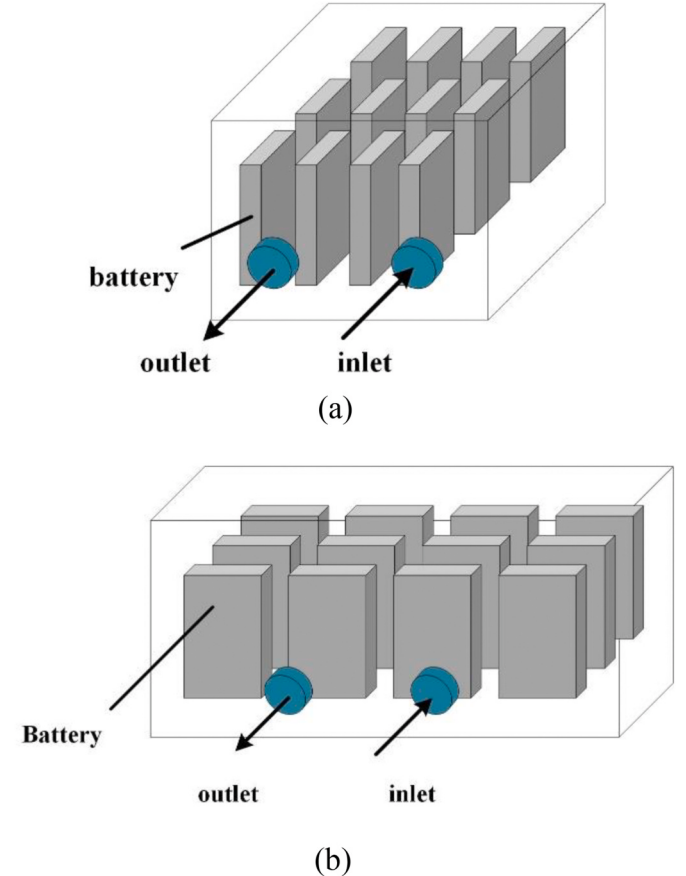


**Fig. 6.** The layouts of battery pack. (a) The vertical battery pack. (b) The horizontal battery pack.

liquid are generally higher than that of air, so the cooling effect of liquid cooling system exceeds that of air-cooling system.

#### 3.2.1. Liquid direct cooling

Liquid cooling is classified into direct-cooling type and indirect-cooling type based on the contact between coolant and battery. For the purpose of preventing short circuit and electrochemical corrosion in the contact between the coolant and the battery, the coolant should be insulated, non-toxic, chemically stable and flame retardant. Silicon oil and mineral oil are mostly selected as coolant in the current research [80]. Immersing the battery pack into coolant liquid cools the entire surface, which helps to improve temperature uniformity and reduce local thermal effects.

Gils and Hirano et al. [81,82] proposed the technology of direct liquid two-phase cooling. They chose Novec7000 of 3 M company (boiling point 34 °C at atmospheric pressure, 99.5%  $C_3F_7OCH_3$ ) as the coolant, as shown in Table 3. Hirano et al. [81] found through experiments that Novec7000 can keep the temperature of battery around 35 °C even at 20C charge/discharge rate. Gils et al. proved that the cooling effect of liquid without boiling exceeded that of air. After the temperature of liquid reached the boiling point, the boiling process can further increase the temperature uniformity in battery module. The boiling process was affected by pressure, so it was necessary to investigate how to control the boiling intensity actively by adjusting the pressure in the boiling chamber [82]. Pendergast et al. [83] placed 18,650 battery modules in an aluminum case and cooled them underwater, demonstrating that water cooling can maintain the temperature of module in normal range. Kim and Pesaran [84] discovered that mineral oil could keep the temperature rise of cylindrical battery and suppress temperature oscillation to a certain extent once high transient heat generated.

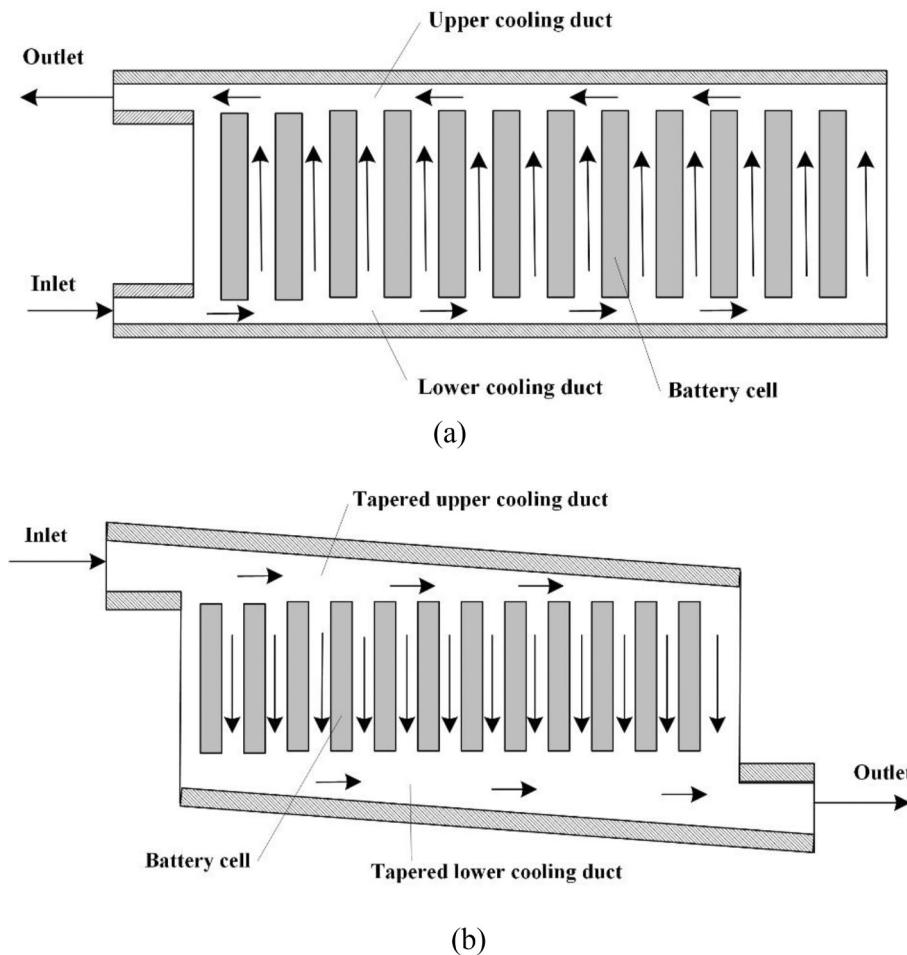


**Fig. 7.** Schematic of battery pack. (a) U-type flow. (b) Z-type flow with tapered cooling duct [69].

**Table 3**  
Thermophysical properties of heat-transfer medium.

Symbol	$\rho$ (kg/m <sup>3</sup> )	$C_p$ (J/kg/K)	$k$ (W/m/K)	$\nu$ (m <sup>2</sup> /s)	$\mu$ (Pa·s)	$T_m$ (°C)
Air [84]	1.225	1006.43	0.0242	1.461e-5	–	–
Mineral oil [84]	924.1	1900	0.13	5.6e-5	–	–
Silicone oil [85]	920	1370	0.15	–	–	–
Water [96]	1000	4200	0.552	5.5e-4	0	–
Water/glycol [84]	1069	3323	0.3892	2.582e-6	–	–
Novec7000 [81,82]	1400	1300	0.075	3.2e-7	–	–
Gallium [95,96]	6093 (33.28 °C)	409.9 (29.8 °C)	29.28 (29.8 °C)	1.89e-3	29.8	–
GaIn <sub>20</sub> [95]	6335 (20 °C)	403.5 (20 °C)	26.58 (20 °C)	–	16	–
Ga <sub>68</sub> In <sub>20</sub> Sn <sub>12</sub> [94]	6363	366	39	2.22e-3	<10	–
Galinstan [97] (66Ga-20.5In-13.5Snwt%)	6440 (20 °C)	290 (20 °C)	16.5 (20 °C)	–	2.4e-3	-19

Karimi [85] and Nelson [86] claimed that silicone oil had a better cooling effect than air. Luo et al. [87] took transformer oil as coolant. Its cooling effect at 4C discharge rate was studied experimentally and numerically. Although the method was feasible, the temperature of transformer oil was not controllable during cooling process. Novec7000 had a high price and the viscosity of oil was generally high. Hence, once the system needed a large coolant flow and velocity, it led to a large pressure loss and power consumption [88]. The pressure drop increased rapidly with the increasing flow rate of coolant. With the same flow rate, the pressure drop in oil-cooling system related to viscosity was several times that in water-cooling system. The oil cooling system shall adopt a low flow rate to reduce the pressure drop. Hence, although the liquid direct cooling systems are available for battery packs, the risk of leakage and the difficulty in controlling the temperature of coolant seriously

restrict the extensive application of direct cooling technology [89].

### 3.2.2. Liquid indirect cooling

To avoid liquid leakage and short circuit, the indirect liquid cooling system mostly uses cold plates, water jackets to contact cells, which are filled with coolant for circulation and heat exchange [90]. The general structure of system is shown in Fig. 8. Liquid pipes are arranged around the cells to carry heat away. The coolant usually transfers the heat to outside by a heat exchanger, and then re-circulates into the cells for heat dissipation. The liquid indirect cooling system requires better airtightness. Additional components such as water jackets and heat exchanger make the system more complex than air-cooling system. These factors lead to increased system weight and maintenance cost [91].

Panchal et al. [92] chose water as the coolant to fill the aluminum

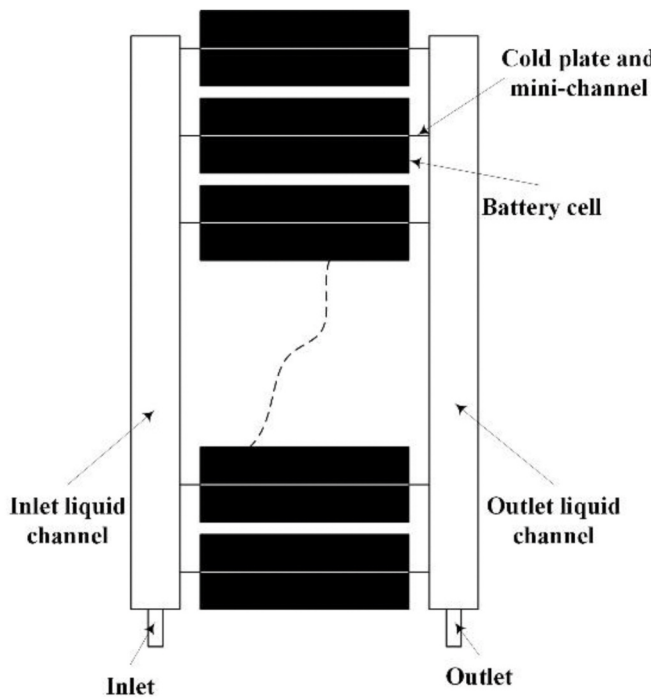


**Fig. 8.** Schematic diagram of liquid indirect cooling system.

cold plates. The neural network approach was introduced to build the thermal model of battery. The cooling effect of water on pouch cells was studied numerically and experimentally. The result showed that water cooling could suppress the maximum temperature and uniformize the temperature field. Wang et al. [93] also believed that water was an effective coolant. They designed a cooling system based on silicon plates and water. The cooling effect was shown to increase with the growth of flow rate. As the flow rate achieved the critical value, the cooling capacity was less affected by the further growth of flow rate because of the limitation of material properties. With the flow rate of 4 mL/s, the maximum temperature in the square battery module didn't exceed 48.7 °C and the temperature difference was less than 5 °C. Water freezes at 0 °C with volume expansion, which limits the application of water-cooling system in cold areas below 0 °C and may even cause safety problems. Glycol is often mixed with water to lower the freezing point to prevent freezing at low temperature. The specific heat capacity and thermal conductivity of the glycol/water mixture are higher than that of air, while the kinematic viscosity is lower than that of oil, as exhibited in Table 3.

Liquid gallium with low viscosity and high thermal conductivity could also be served as the heat-transfer medium. Some researchers have carried out a series of studies on liquid metals. Yang et al. [94] presented a liquid-cooling system with gallium, Ga<sub>80</sub>In<sub>20</sub> and Ga<sub>68</sub>In<sub>20</sub>Sn<sub>12</sub> as coolants. They evaluated performance indicators such as cooling capacity, pump power consumption and temperature uniformity, and compared them with water-cooling system. The liquid metal can achieve lower and more uniform temperatures, as well as lower pump power consumption with same flow condition. They argued that liquid metal could handle complex thermal conditions like high power, high environment temperatures or battery failures. Liquid metals are electrically conductive, which means that an electromagnetic pump can be considered to drive the liquid metals [95]. As Table 3 showed, the melting points of liquid metal are mostly within the working temperature range of battery. The volume change during phase transition should be paid attention to avoid damaging the battery. The widespread use of liquid metals is also limited by high prices.

Many researchers take optimizing channel design as their research direction to improve cooling performance. The liquid-channel design of

indirect cooling system is diversified, such as cold plate type, fin type and microchannel type. Fig. 9(a) presents a typical structure of pouch battery pack with fins and cold plates. The fins facilitate the redistribution of local high temperature heat flow in battery pack, thus reducing the temperature difference at individual cell level. However, as the liquid flows through each fin successively, the temperature difference between liquid and fins decreases gradually, and the cooling performance decreases. Chung and Kim [98] introduced the equivalent thermal conductivity, and numerically analyzed the factors affecting the cooling performance and temperature uniformity from the inside cell, cells and module. The result proved that the poor heat conducting efficiency between the undersurface of the battery module and cold plates was the main reason affecting the heat dissipation, and the unsymmetrical structure also reduced the temperature uniformity.

The coolant simultaneously flows to the mini-channel cold plates with high thermal conductivity attached among cells, in the BTMS shown in Fig. 9(b). This system allows for even temperature distribution. Nevertheless, due to the long and narrow mini channel, the pressure drop in channels is high, which requires a high-power pump to drive the coolant circulation and consumes. A mini-channel liquid cooling system with oblique fins was developed in Ref. [99], and its cooling capacity was proved to be superior to the system with traditional straight channel cold plates through experiments. When the thermal load was 220 W and 1240 W, the battery temperature didn't exceed 50 °C under the flow rate of 0.1 L/min and 0.9 L/min. Zhao et al. [100] worked on the influence of several parameters on the cooling performance of the micro-channel liquid cooling system. The simulation result indicated that when the channel number exceeded 4, and the inlet mass flow was 10<sup>-3</sup> kg/s, the maximum temperature in the cylindrical battery pack was able to controlled no higher than 40 °C. Considering the maximum temperature and local temperature difference, this system was superior to natural convection cooling only if the channel number exceeded 8. Qian et al. [101] adopted a liquid cooling method based on microchannel and established a 3D model. They also analyzed the effects of channel number, inlet mass flow, channel flow direction as well channel width on the temperature field. The microchannel liquid system suppressed the surface temperature during 5C discharging and was also effective to increase the inlet mass flow.

As pictured in Fig. 9(c), the snake-shaped channel liquid-cooled system also drew the attention for increasing the heat transfer area. Jarrett and Kim [102] modeled and investigated the characteristics of the serpentine-shaped channel cooling plate by CFD method. They defined objective functions for pressure drop, average temperature, temperature uniformity, and then numerically optimized them by changing channel width and position. The optimization methods of the lowest average temperature and pressure drop were basically the same, namely the widest channel possible. A narrower inlet and a wider outlet contributed to more even temperature field. Zhao et al. [103] worked on the temperature uniformity in battery pack under serpentine-channels liquid cooling through simulation. The nonuniformity of temperature field was reduced by shortening the flow path with multi-serpentine channels and increasing the contact area among cells and the serpentine channels along the flow direction. These two methods kept the temperature difference below 2.2 K and 0.7 K respectively in the process of 5C discharge rate. The cold plates with u-shaped serpentine channels was established in Ref. [104] and the impacts of the channels number, channel arrangement and inlet temperature of coolant on the BTMS were studied numerically. The optimal cooling performance can be achieved with five channels in the length direction. The five-channel arrangement in length flow direction can reduce the maximum temperature by 26 °C compared with the two-channel arrangement in width flow direction. Whereas considering the efficiency and safety of the BTMS, the channels number and inlet temperature are capped.

Some scholars increase the contact area by combining the thermal conductive silicone sheet and metal plate with the liquid pipeline, so as to promote the adaptability of liquid-based BTMS to the shapes of

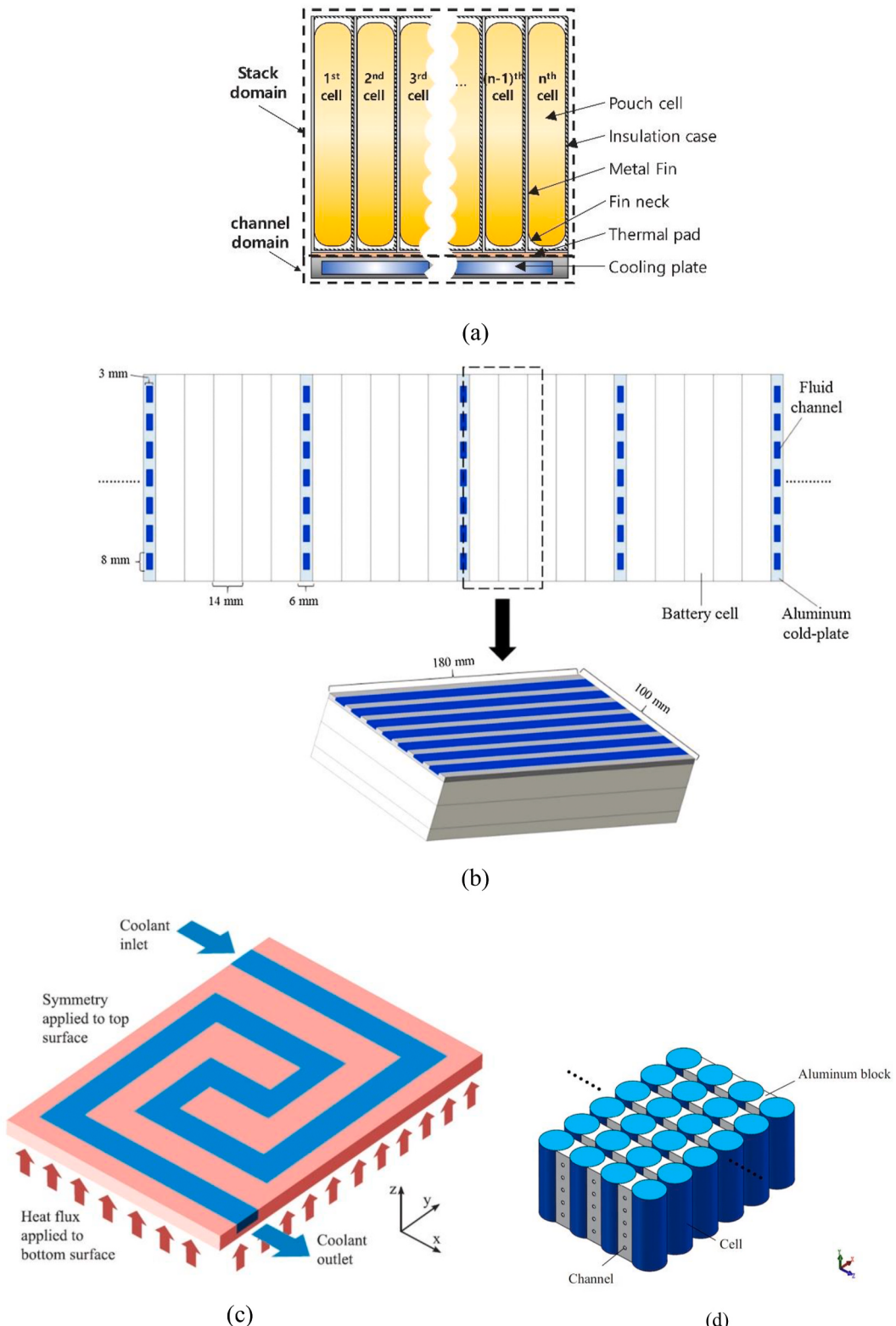


**Fig. 9.** Schematic diagram of liquid cooling system. (a) Finned liquid cooling system [98]. (b) mini-channel liquid cooling system [106]. (c) liquid cooling system with serpentine channels [102]. (d) Liquid cooling system with aluminum blocks [105].

batteries. Rao et al. [105] combined the aluminum block with the cooling channels to enlarge the heat-transfer region between the liquid BTMS and cylindrical batteries, and simulated the influence of length and speed of the aluminum block on the temperature field, as shown in Fig. 9(d). Aluminum blocks can quickly transfer heat to water. When the

lengths of the heat transfer regions to each cell were equal, the maximum temperature decreased as the inlet velocity increased. Because of the temperature gradient in the heat transfer process of water, the temperature field in the module was not even. The further away from the inlet, the greater the temperature difference. So, they

designed the contact length increasing linearly with the distance of cells from the inlet, thereby enlarging the heat exchange area of the cell at the far end of the inlet and promoting the evenness of temperature field. The thermal conductive silicone sheet was combined with water channels to increase the heat exchange area in Ref. [93], and it was proved through experiments that the thermal conductive silicone sheet effectively enhanced the heat dissipation in the water-based BTMS.

In conclusion, the shape of the liquid channel, the channels number, channel layout, flow direction and inlet size all affect the thermal behavior of BTMS. The temperature field is directly affected by the liquid flow path and the contact area between batteries and channels, while the heat exchange capacity between liquid and batteries are affected by the shape and area of channels.

### 3.3. PCM cooling system

The physical state of PCM varies with temperature. Phase transitions include solid-liquid, gas-liquid, and solid-gas. The material absorbs or exotherms heat when the phase changes, but the temperature changes little. Organic solid-liquid PCMs have the advantages of small volume change, large latent heat and good thermal stability during phase transition, which make them the preferred choice of energy storage materials. The thermophysical properties are shown in Table 4.

PCMs cooling system uses the heat storage process of PCMs to realize the heat dissipation of lithium-ion battery without extra power consumption, which belongs to passive cooling [110], as Fig. 10 showed. As the initial temperature doesn't reach the melting point, PCM absorbs heat with sensible heat. As the temperature gradually rises to the melting point, PCM begins to melt and absorbs heat as latent heat. The temperature changes very little until the phase transition is over. Thus, PCM cooling could manage the severe thermal conditions happened to battery pack [111].

For ideal battery PCM, on the basis of nontoxicity and non-corrosiveness, the latent heat, specific heat capacity and thermal conductivity ought to be large, and the phase transition temperature ought to be in the normal temperature range of the battery. As exhibited in Table 4, paraffin is currently used as PCM for BTMS, because of its low price, good thermal stability, non-corrosive, small volume change rate and large latent heat, whereas a significant defect of paraffin is low

thermal conductivity. It directly affects the cooling efficiency of BTMS [113]. Thus, how to strengthen heat transfer is one of the hotspots.

#### 3.3.1. Preparation of composite phase change material (CPCM)

Many studies have focused on the preparation of CPCMs to improve thermal conductivity. The composition and thermophysical properties of CPCMs are exhibited in Table 5. Zhang et al. [114] prepared expanded graphite (EG)/paraffin CPCM by absorbing liquid paraffin into EG and investigated its properties experimentally. EG prepared at 800 W power radiation for 10s had the highest adsorption capacity of paraffin (92 wt %). Differential scanning calorimetry (DSC) analysis indicated that the solid-liquid phase transition temperature of CPCM (52.2 °C) was near that of paraffin (52.5 °C). The latent heat of CPCM (170.3 J/g) was the product of the latent heat of paraffin (188.2 J/g) and the mass fraction (92 wt%). Paraffin and EG were combined to obtain CPCM, and no new substances were demonstrated to be produced by X-Ray diffraction (XRD). Jiang et al. [115] demonstrated that adsorbing paraffin into EG improved the heat transfer in CPCM. They compared the cooling characteristics of PCM mixed EG in various proportions. Considering that the leakage risk of liquid paraffin reduced with the increasing mass fraction of EG, the CPCM with 16–20 wt% EG is preferred for BTMS. Rao et al. [116] designed a BTMS based on paraffin/copper foam (CF) CPCM and discussed the temperature difference and distribution by experiments. The discharge current was positively correlated with the local temperature difference among cells increased, and the local temperature difference fluctuated significantly during the driving process of EV. The maximum temperature and local temperature difference were kept lower than 45 °C and 5 °C separately under the constant-current discharge condition and below 40 °C and 3 °C at road operation.

Wu et al. [117] developed a copper mesh-paraffin/EG CPCM. The results showed that heat transfer, strength and temperature uniformity in CPCM can be enhanced by adding copper mesh. Lv et al. [118] built a BTMS based on ternary CPCM of EG, paraffin and low-density polyethylene (LDPE), combining aluminum fins (Fig. 11). The LDPE frame improved mechanical molding performance and prevented liquid paraffin leaking in certain degree. Coupled low fins enhanced the surface heat transfer capability. The ternary CPCM had better mechanical properties. The maximum temperature and temperature difference were kept lower than 50 °C and 5 °C at 3.5C discharge rate through ternary CPCM coupled fins. He et al. [119] also developed a ternary CPCM for BTMS, which was prepared by coupling the EG/CF skeleton with paraffin. EG adsorbed paraffin and transferred heat to the adjacent CF frame through its conductive porous structure. As a macro skeleton, CF transferred heat to the whole CPCM, which enhanced the interface heat transfer. The EG/CF skeleton was proved to strengthen the CPCM structure. Zhang et al. [120] prepared a novel ternary CPCM with kaolin/EG/paraffin. They compared the thermal properties of ternary composites with different proportions and indicated that the ternary composites with 10 wt%EG and 10 wt% kaolin had better temperature control performance.

Hussain et al. [121] developed a BTMS based on nickel foam (NF)/paraffin CPCM. The maximum temperature can be reduced by 24% at 2C discharge rate compared with paraffin. The battery temperature was positively correlated with the pore density and porosity of NF. Azizi and Sadrameli [122] prepared aluminum wire mesh/Poly Ethylene Glycol 1000(PEG1000) CPCM for LiFePO<sub>4</sub> battery pack by selecting PEG1000 with melting point of 35 ~ 40 °C as PCM. The maximum surface temperatures of cells decreased by 19%, 21% and 26% at the discharge rates of 1C, 2C and 3C, respectively. The application of aluminum foam (Al-foam)/paraffin CPCM in BTMS was researched in Refs. [113,123], and it was proved that the CPCM had higher thermal conductivity than paraffin. Zou et al. [124] prepared a new type of CPCM by adding graphene, carbon tube and EG into paraffin, which could prevent liquid PCM leaking. Moreover, its local heat transfer effect in a limited area under different thermal environment was almost the same as that of the CF/paraffin. Goli et al. [125] demonstrated graphene

**Table 4**  
Thermophysical parameters of several PCMs.

Symbol	$\rho$ (kg/m <sup>3</sup> )	k (W/m/K)	H (kJ/kg)	T <sub>m</sub> (°C)
Paraffin C <sub>13</sub> –C <sub>24</sub> [107]	0.76 (liquid, 70 °C); 0.9 (solid, 20 °C);	0.21 (solid)	189	22–24
1-Dodecanol [107]	–	–	200	26
Paraffin C <sub>16</sub> –C <sub>28</sub> [107]	0.765 (liquid, 70 °C); 0.910 (solid, 20 °C);	0.21	189	42–44
Paraffin C <sub>20</sub> –C <sub>33</sub> [107]	0.769 (liquid, 70 °C); 0.912 (solid, 20 °C);	0.21	189	48–50
Paraffin C <sub>22</sub> –C <sub>45</sub> [107]	0.795 (liquid, 70 °C); 0.920 (solid, 20 °C);	0.21	189	58–60
1-Tetradecanol [107]	–	–	205	38
Stearic acid [108]	–	–	224.3	67.7
n-docosane [109]	771 (liquid) 791 (solid)	0.15 (liquid) 0.21 (solid)	249	44–46
n-tetracosane [109]	770 (liquid) 796 (solid)	0.15 (liquid) 0.21 (solid)	255	50–52
n-pentacosane [109]	724 (liquid) 814 (solid)	0.152 (liquid) 0.21 (solid)	235	54–57

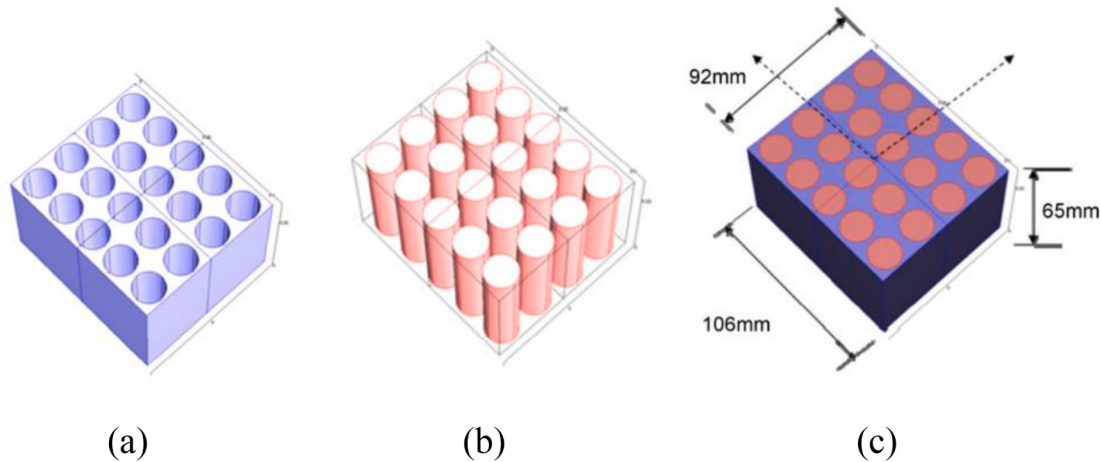


**Fig. 10.** Schematic diagram of PCM-based BTMS. (a) PCM filled box. (b) Cell layout. (c) Battery module [112].

**Table 5**  
Thermophysical parameters of composite PCMs.

	$\rho$ (kg/m <sup>3</sup> )	k(W/m/K)	H (kJ/kg)	T <sub>m</sub> (°C)
Paraffin/graphite powder (mass ratio 4:1) [129]	–	7.3	162	49.8
Paraffin/EG (92 wt% paraffin) [114]	–	–	170.3	52.2
Copper mesh-paraffin/EG [117]	–	7.65	141.6	42
EG/paraffin/LDPE [118]	856	1.38	87.4	44.5–50.2
(10 wt%)kaolin/(10 wt%) EG/paraffin [120]	–	7.5	165.21	37.87
(30 °C)				
Nickel foam/paraffin [121]	–	1.16	–	38–41
Al-foam/paraffin [123]	805	–	120	55–60
Graphene/carbon tube/EG/paraffin [124]	–	5.1	178.5	46.1
Graphite matrix/paraffin [130]	789	16.6	185	42–45
EG/paraffin (T <sub>m</sub> of paraffin:37 °C,48 °C,55 °C) [131]	–	5–25	156 (37 °C);153 (48 °C);183 (55 °C)	37 (37 °C);55 (48 °C);67 (55 °C)
EG/graphite sheets/paraffin [132]	842	3.95	132.6	21.6–25.5
Octadecane/Al-foam (0.88 porosity) [133]	–	24.97 (liquid); 25.15 (solid)	243.5	–
Copper foam/paraffin [134]	–	3.112	170.4	48



**Fig. 11.** Battery pack coupling EG/paraffin/LDPE composite PCM with low fins [118].

strengthened the heat transfer in paraffin-based CPCM too. Coupling graphene to paraffin increased the thermal conductivity of CPCM by at least two orders of magnitude without losing the energy storage capacity. The heat transfer enhancement of graphene coated NF on PCM was investigated in Refs. [126,127]. The graphene/NF/paraffin composites decreased the temperature rise of cells by 17% compared with NF/paraffin composites at 1.7 A discharge current. The thermal conductivity of paraffin increased 23 times after adding graphene coated

NF.

Wu et al. [128] established a 3D thermal model for the rectangular battery with multilayer structure and studied the influence of PCM thickness and convection heat-transfer coefficient on temperature field. The temperature gradient of the battery was negatively correlated with PCM thickness. Whereas, because of the low heat transfer efficiency inside battery, increasing the convective heat transfer coefficient had limited influence on the temperature-gradient decrease. The marginal PCM thickness as well convection heat-transfer coefficient around the battery were helpful for optimizing the system. Phase transition completed basically at the marginal value. When the two parameters were different from the marginal value, the temperature distribution was significantly different.

Although adding high thermal conductivity materials (graphene, metal foam, EG, etc.) into the PCMs can enhance the thermal conductivity, thermal runaway may be caused by the complete melting of PCMs and loss of heat storage capacity in the continuous charging and discharging cycle of large current, which is difficult to meet the cooling requirements of battery packs. Additional cooling methods are needed to assist heat dissipation to ensure the heat dissipation effect under extreme conditions. Hence, the active BTMS combining PCMs with forced heat transfer has gradually become one of the research directions. PCMs are mainly utilized to suppress the temperature rise of batteries, while forced cooling system strengthens the heat transfer from PCMs to outside.

### 3.3.2. Forced air convection-PCM

As shown in Fig. 12, Fathabadi [135] proposed an active-passive hybrid BTMS scheme for battery pack. The active part took air cooling technology to dissipate heat through distributed air ducts, while the

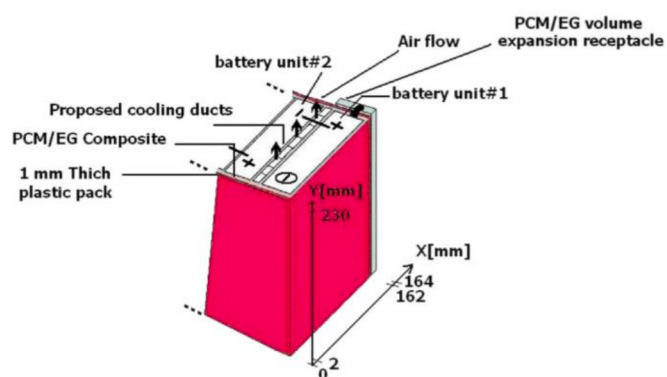


**Fig. 12.** Active-passive hybrid BTMS [135].

passive part took paraffin/EG CPCM to optimize the thermal performance. They conducted simulation on the temperature field at different ambient temperatures, and found that the BTMS could keep the maximum temperature below 60 °C even with the ambient temperature of 55 °C. Ling et al. [136] also proposed an active-passive hybrid system (Fig. 13) combining RT44HC/EG with forced air cooling, and compared with RT44HC/EG CPCM. The passive part (RT44HC/EG) can only ensure the battery temperature below 60 °C in the first two cycles at 1.5C and 2C discharge cycles. The hybrid BTMS controlled the maximum temperature below 50 °C in any cycle not exceeding 2C discharge rate. They believed that thermal properties of PCM determined the maximum and evenness of the temperature field, and forced air convection contributed to the recovery of heat storage capacity. Hence, the integration of PCM with the air-cooling system improved the reliability of BTMS.

### 3.3.3. Fins-PCM

Metal has good thermal conductivity. Setting metal fins in PCMs can enlarge the heat-transfer area, which has been one of the hot spots that researchers pay attention to. The main research direction focuses on optimizing the size, shape and arrangement of fins.

With stearic acid as PCM, Liu et al. [108] designed spiral twisted copper fins to be fixed on the electric heating rod to improve the thermal response rate of PCM in an annulus. Copper fins enhanced the equivalent thermal conductivity of stearic acid-based system by 1–3 times. The equivalent thermal conductivity was increased by 67% during pre-melting stage. As PCM continued melting, the heat conduction enhancement was gradually obvious. They demonstrated that decreasing the fin width was beneficial to improving the equivalent thermal conductivity, and decreasing the spacing of fins was beneficial to accelerating melting. Ping et al. [109] proposed a hybrid BTMS integrated with PCMs and fins to decrease the battery temperature at high-temperature environment (40 °C) and improve the temperature uniformity. Three types of materials, including n-docosane, n-tetracosane and n-pentacosane were chosen to be PCMs. The influence of material type, fin size, spacing between fins and PCM thickness on the temperature field were researched through simulation and the experimental data proved that the optimized design of PCM-fins BTMS was able to keep the maximum temperature below 51 °C at 3C discharge rate.

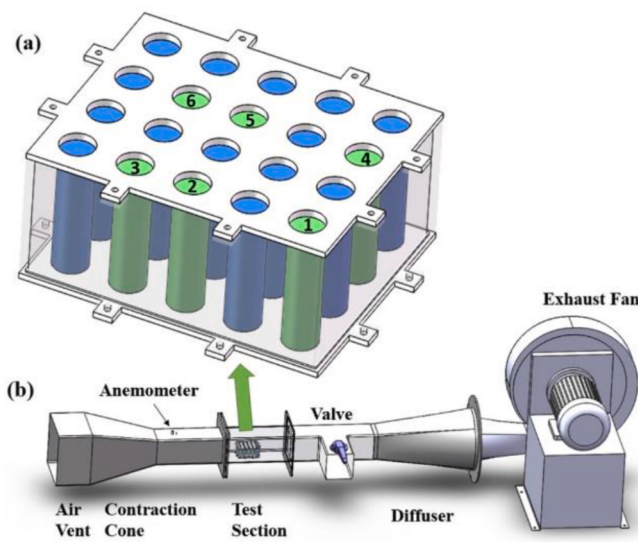


**Fig. 13.** Schematic of active-passive hybrid BTMS: (a) A 5S4P battery pack containing six temperature measure points (marked in green); (b) Structure of the air channel [136]. (For interpretation of the references to colour in this figure legend, the reader is referred to the Web version of this article.)

Weng et al. [137] discussed the influence of aluminum alloy fins shape on PCM-BTMS for cylindrical battery by contrast experiments of with and without fins. The longitudinal fins helped to enhance the heat convection between air and environment, while the circular fins enhanced the thermal conductivity inside PCM due to its large surface area. Adding fins in finite space didn't necessarily increase the heat transfer efficiency of fins. The experiment proved that the BTMS with four longitudinal fins reduced the battery temperature from 36.9 °C to 34.2 °C. They designed an optimized PCM-fins module with two circular fins at the bottom and four rectangular fins at the top. The maximum temperature of the optimized module was 29.1 °C at 1C charging rate, which was 5.5% lower than the rectangular finned module. The experimental research provided ideas for the design of the PCM based fin module.

### 3.4. HP cooling system

As a kind of high efficiency heat conduction element with phase change medium, HP is extensively applied in the areas of industry, military, as well radiator. It is drawn into negative pressure and injected into working medium with low boiling point. It is generally divided into evaporator, adiabatic and condenser sections along the axial direction, as shown in Fig. 14(a). The working medium vaporizes in evaporator

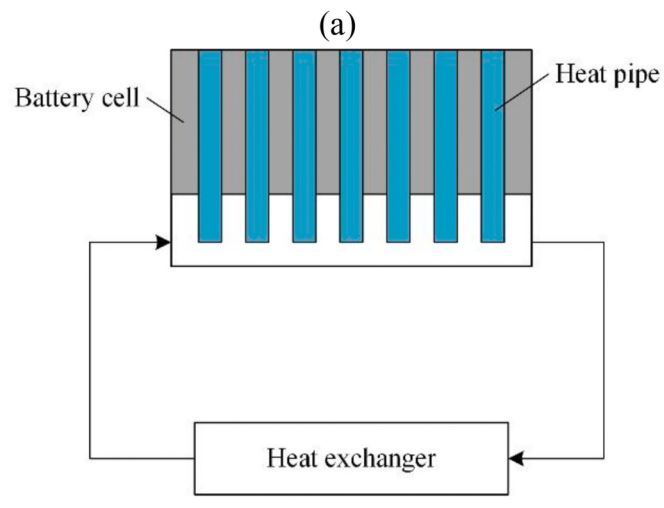
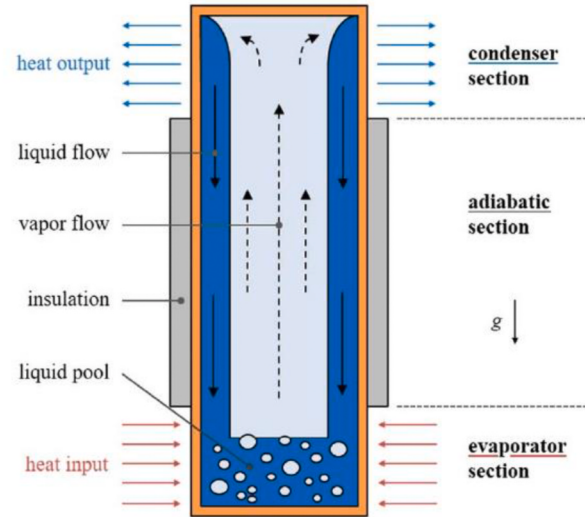


**Fig. 14.** BTMS based on HP. (a) Operating principle of HP [139]. (b) Schematic diagram of HP cooling system [140].

section, then enters the condenser section. The working medium condenses into liquid by heat exchange between the condenser section and external environment, and then flows back to the evaporator section through suction core. Thus, efficient heat transfer is carried out through the reciprocating cycle of working medium and phase transition. The evaporator section is usually connected to heat sources. Depending on the driving force, the working medium can flow back to the evaporator section in various ways [138]. As shown in Fig. 14(b), the evaporator section is coupled with cold plates to absorb the heat of battery, and then extends through the condenser section to the outside of battery module exchange heat with air or liquid.

The temperature and strain in battery pack based on heat pipe cooling device (HPCD) was investigated in Ref. [141]. They were significantly different with different cooling devices under various working conditions, as Fig. 15 exhibited. The battery temperature under natural convection was too high when the discharge ended. HPCD reduced the temperature rise and strain effectively at room temperature. Compared with the ambient cooling, the HPCD system with fan decreased the maximum temperature by 15 °C and the strain value by 50% at 1C discharge rate. Liang et al. [142] discussed the influence of coolant flow, ambient temperature, coolant temperature and start-up time on the temperature field in HP-BTMS. When the ambient temperature was below 25 °C, the cooling capacity of HP-BTMS improved slightly as the ambient temperature went down. Lowering the coolant temperature could maintain the cooling capacity of the system basically unchanged at ambient temperature below 35 °C. The maximum temperature and temperature difference were controlled well with intermittent cooling. There was no significant difference in the response of intermittent cooling and continuous cooling to battery temperature. Therefore, it is feasible to decrease the power consumption of the system through shortening the running time.

HP can be used as a cooling medium to cool battery packs alone or as an auxiliary device for forced cooling of PCMs, rapidly transferring the heat absorbed by PCMs. Zhao et al. [143] designed a PCM/HP coupling BTMS and carried out experiments, as pictured in Fig. 16. The PCM/HP

coupled BTMS kept the maximum temperature below 50 °C longer than PCM under the same condition. Compared with air natural convection, PCM reduced the temperature difference by about 33.6%, while embedding HP into PCM further reduced the temperature difference by 28.9%. The coupled BTMS kept the maximum temperature difference below 5 °C longer than air natural convection and PCM. Wu et al. [144] also designed a BTMS based on HP/PCM. The experimental results proved that HP affected the temperature distribution uniformity at high discharge rate. The maximum temperature was maintained lower than 50 °C even at high discharge rate of 5C under forced air convection. The temperature fluctuation is smaller under cyclic conditions. The PCM/oscillating heat pipe (OHP) BTMS was constructed in Ref. [145], as shown in Fig. 17. They put electric heating rods into aluminum blocks instead of square batteries. The temperature variation of aluminum blocks under different power was discussed. The influence of various factors such as terminal direction and OHP layout of aluminum block was analyzed. For the purpose of acquiring the even temperature field, the starting temperature of OHP cannot exceed the phase transition temperature of PCM, and the terminal of surrogate battery should be far away from the adiabatic section.

In conclusion, HP is effective in enhancing the heat transfer of PCMs, but it may lead to complex structure and large volume of BTMS. The coupling mechanism between air cooling, PCM and HP remains to be further studied, which will become one of the trends in the application of HP to BTMS [146,147]. Table 6 compared and evaluated various cooling methods from multiple perspectives.

### 3.5. Preheating of BTMS at low temperature

Scholars have conducted studies on thermal management in different directions so far, many of which focus on controlling temperature rise during charging and discharging by using air or coolant. However, EVs need to be able to operate at low temperatures as well as high temperatures, just like gasoline cars. Lithium-ion battery is a charge and discharge device through electrochemical reaction. At low ambient

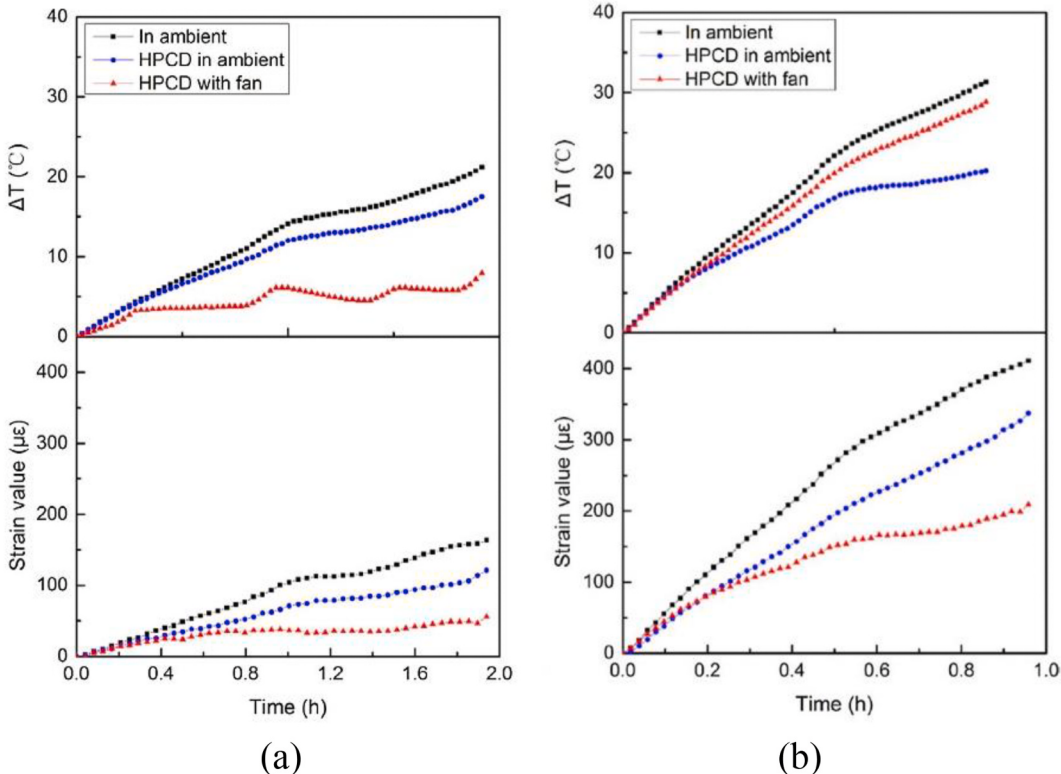


**Fig. 15.** The center temperature rise and strain value of battery pack with different cooling devices at the discharge rate of (a) 0.5C and (b) 1C [141].

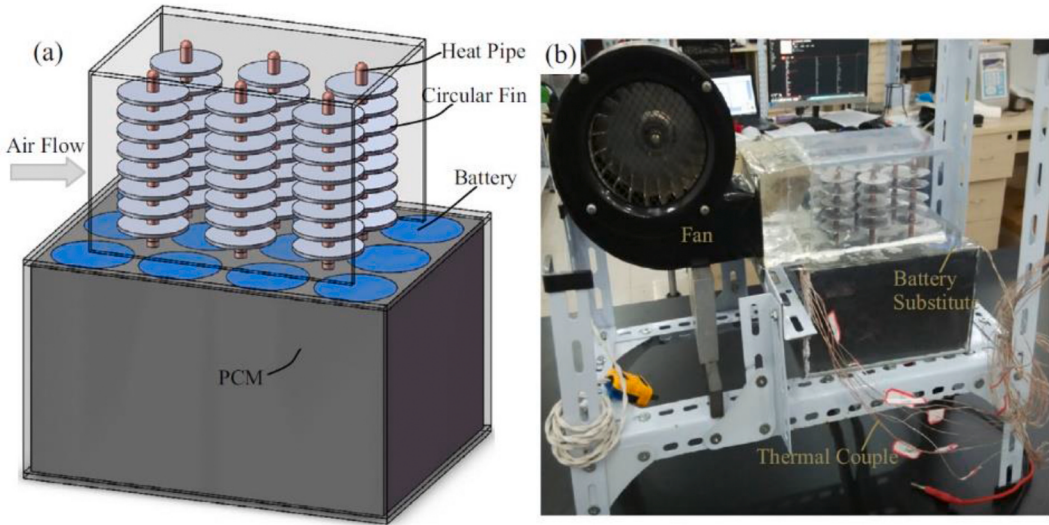


**Fig. 16.** BTMS based on HP and PCM: (a) Structure diagram; (b) Actual photo [143].

temperature, the internal resistance increases and the chemical activity decreases, causing battery capacity degradation. The charging capacity of low temperature environment is smaller than that of room temperature environment at the same charging current and time. In addition, if the battery is used for a long time without preheating at low temperature, the performance and life will be damaged [148,149]. The electricity and energy required by the vehicle cannot be transferred efficiently, especially if the vehicle is parked for a long time. Therefore, BTMS that can rapidly preheat the battery to normal temperature at low temperatures is necessary.

### 3.6. Internal heating

#### 3.6.1. Direct current (DC) heating of battery internal resistance

The electrochemical reactions interact with the thermal characteristics of batteries. The electrochemical reaction heat and the heat exchange with surrounding environment determines the change in battery temperature. While the dynamic process and transport characteristics inside battery are affected by temperature, which further influences the electrochemical reactions [150,151]. The ionic diffusivity, electrolyte conductivity and lithium ion diffusivity of the anode decrease at low temperature, which affects the electrochemical performance of the battery. As the internal resistance increases, the available capacity decreases [152–154]. At the same time, the increase in internal resistance leads to more internal heat generation. Lu et al. [155] demonstrated that the charging and discharging performance of the battery with  $\text{Li}(\text{Ni}_x\text{Co}_y\text{Al}_z)\text{O}_2$  cathode decreased sharply below 20 °C. Although the heat generated by batteries may accelerate the degradation during cycles, the discharge characteristics can also be improved within the appropriate temperature range, which means that lithium-ion battery can recover battery performance by preheating with internal resistance at low temperatures.

Ji et al. [156] discharged the batteries at constant current and constant voltage respectively until the temperature reached 20 °C, and studied the effect of discharge strategy on temperature. As Fig. 18 exhibited, the maximum temperature rising rate appeared in the early constant-current discharging, while the temperature rising rate increased gradually in the constant-voltage discharging. The advantage of internal resistance heating is high heating efficiency, avoiding heat loss caused by heat conduction from the outside to the batteries. High power conditions are optional when rapid heating is required. However, attention should be paid to capacity attenuation caused by lithium precipitation at low temperature to avoid battery aging [157,158].

#### 3.6.2. Pulse heating of internal-resistance

Qu et al. [159] found through experiments that only 175s was needed for the battery to be heated to 10 °C at -10 °C in the pulse heating mode, and 280s was needed in the continuous DC heating mode. An alternating current (AC) pulse internal-heating system was developed in Ref. [160]. Its feasibility was verified by conducting AC pulse-heating cycles and low-temperature charging experiments on 30Ah pouch LiFePO<sub>4</sub> battery pack. The high current amplitude was beneficial for energy storage and temperature raise, and the temperature uniformity between the surface and inside battery was good during AC heating. After hundreds of cycles, the performance of batteries didn't decline significantly, which proved that the system had potential application value in cold environments. Zhang et al. [161] constructed sinusoidal AC internal preheating system for 18,650 batteries at low temperature and predicted the temperature rise by lumped energy conservation model. The reliability of the model was verified by pre-heating experiments under different insulation conditions. The heating rate was positively correlated with the amplitude and thermal insulation, but negatively correlated with the frequency. No significant capacity loss was found after repeated tests. They demonstrated that the model had high computational efficiency and was beneficial for real-time control of automobile preheating device. Zhao et al. [162] also proposed a low-temperature pulse charging method. Before conventional constant-current and constant-voltage charging, LiFePO<sub>4</sub>/C batteries were excited by a pulse current with charging ratio of 0.5~2C and discharge ratio of 3~4C. Compared with the conventional constant current-voltage charging-discharging cycles, the total charging time was shortened by 36 min (23.4%) and the charging capacity increased by 7.1% under the same working conditions and ambient temperature.

Ji et al. [156] separated cells into two groups with equal capacity and opposite charging-discharging states (Fig. 19). The output power of the discharge group was the input power of the charging group. A dc-dc converter was set to amplify the output voltage to meet the required voltage for charging. The charging and discharging states were switched periodically by pulse signal to balance the charge state of the two groups. The system didn't require any moving parts and had no external heating elements, making it more reliable. The temperature was more evenly distributed too. Whereas, the mutual pulse heating required special circuits and control systems, which increased the cost. Ruan et al. [163] demonstrated an internal preheating system on the basis of electrothermal coupling model. A good balance was achieved between short heating time and small battery life loss by controlling the constant polarization voltage during heating. The heating time and efficiency of

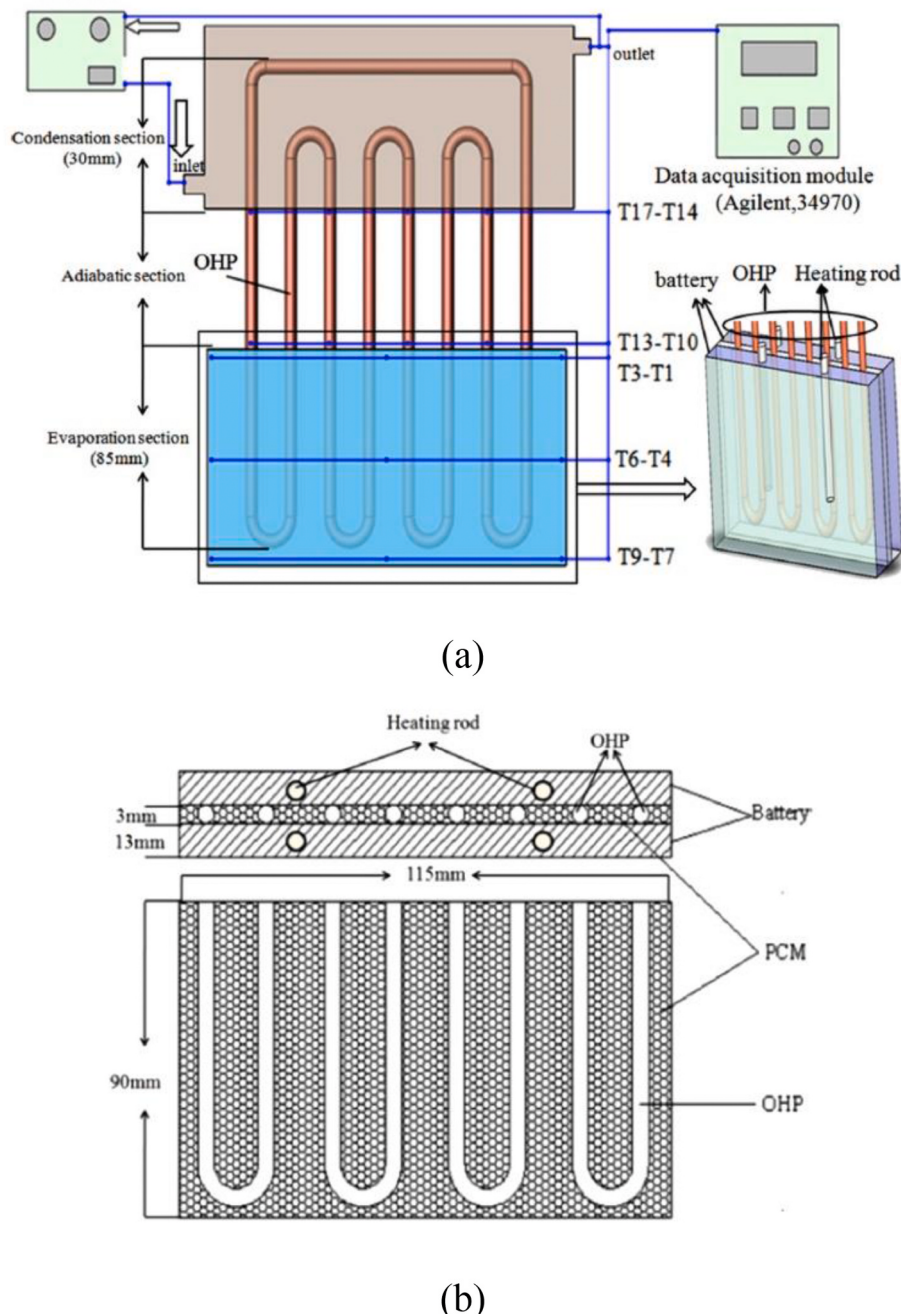


**Fig. 17.** Schematic of PCM/OHP BTMS. (a) OHP battery cooling system. (b) OHP/PCM battery cooling system [145].

variable frequency heating were in line with those of constant frequency heating. However, due to the engineering difficulty of realizing variable frequency heating, constant frequency heating is considered to be more potential.

### 3.6.3. Self heating lithium-ion battery (SHLB)

For the low heat-transfer efficiency between the multi-layer electrode and separator, there is temperature gradient along the thickness during heating in battery at low temperature. Thus, it's impossible to completely eliminate the temperature gradient only by heating with an external heat source. Wang et al. [164] proposed the concept of inserting metal foil into batteries to form SHLB. Without external heating equipment or electrolyte additives, the self-preheating was enabled through closing the switch between the activation terminal and the negative terminal. The results suggested that the preheating time from  $-20^{\circ}\text{C}$  to

$-30^{\circ}\text{C}-0^{\circ}\text{C}$  was 20s and 30s respectively, consuming only 3.8% and 5.5% of the battery capacity. Fig. 20(a) illustrated the structure of SHLB. In addition to anode, cathode, and electrolyte/diaphragm, a layer of nickel foil coated with electrically insulating polymer was inserted in SHLB. The two ends of the foil were the negative and activation terminals respectively. The principle of SHLB was illustrated by the circuit diagram in Fig. 20(b). The switch was opened to force the current to pass through the foil, which produced ohmic heat. The switch turned off to stop heating as the battery temperature exceeded  $0^{\circ}\text{C}$ . Zhang et al. [165] proved through experiments that the nickel foil embedded in SHLB took leading position during self-heating, and the design with two pieces of nickel foil could significantly accelerate the spontaneous heating. They also believed that the nickel foil may also act as an internal temperature sensor because of the linear relation between nickel-foil resistance and temperature.

**Table 6**  
Comparison and evaluation of different battery cooling methods.

	Forced air	Liquid direct	Liquid indirect	PCM	Heat Pipe
Initial cost	Middle	Middle	High	Low	Middle
Maintenance	Easy	Easy	Hard	Easy	Hard
Major components	Fans	–	Pumps, Cold plate, Water jacket	–	Heat pipes
Extra weight	Light	Middle	Heavy	Middle	Heavy
Space requirement	High	Low	High	Low	High
Complexity	Complex	Simple	Complex	Simple	Complex
Shape adaptation	All types	All types	All types	All types	More suitable for prismatic cells
Temperature gradient	High	Middle	Low	Low	Middle
Energy storage capacity	No	No	No	Yes	No
Leakage possibility	No	Yes	Yes	After melting	No
Insulation/heating	Yes	No	Yes	Yes	Yes
Commercialization	Yes	No	Yes	No	No

Yang et al. [166] proposed and verified an electrochemical thermal coupling model for SHLB and predicted its internal characteristics. They suggested that the temperature gradient inside battery was a key factor affecting the self-heating time. A single nickel foil led to large temperature gradient, while two or three pieces reduced the internal temperature gradient, shortened the self-heating time, and reduced the energy consumption by 25%~30%. Yang et al. [167] also compared internal resistance heating and external heater with SHLB, especially on the heating speed and local maximum temperature. The efficiency of internal resistance heating was largely limited by the electric-thermal conversion efficiency. Increasing the power of external heater may cause local overheating, so the heating speed was limited to about 20min for a temperature rise of 30 °C especially for large batteries. The heating speed of SHLB can reach 1~2 °C/s by contrast. Lei et al. [168, 169] established a 3D finite element heating model and analyzed the temperature gradient in the heating process of SHLB. They proposed the intermittent heating method and suggested the appropriate heating time and stop time. For example, after heating 0.1s and stop heating 0.3s, which reduced the temperature difference from 10~11 K to 2~3 K. They also numerically analyzed the influence factors of temperature uniformity, and it was found that reducing heating power and battery thickness could effectively increase the temperature uniformity during heating. SHLB required changing the structure of lithium-ion battery,

but EVs always operated in complex environments and operating conditions, so the safety of SHLB should be carefully considered.

### 3.7. External heating

When batteries are preheated by an external element, the heat source may be heating plates in contact with the batteries or hot fluid (gas or liquid) passing over the battery surface, or a sealed enclosure with an internal heating element. These methods usually use separate power supply for the heating elements.

#### 3.7.1. Heating with external heat source

Resistance heater is one of the common external heat sources. For example, Li et al. [170] used an aluminum plate twined with positive temperature coefficient (PTC) resistance wire for preheating. The convection heating system needs to be closed, including flow channels, heaters, fans and other control elements, as exhibited in Fig. 21. Song et al. [171] conducted heating on the battery through external air convection, and demonstrated that the battery capacity decreased by 3.1% at low temperature without preheating measures.

Fan et al. [172] simulated the ambient temperature of –20 °C and discussed the factors influencing the heating performance of BTMS based on heat plates. The results indicated that the effect of discharge rate on temperature rise was negligible compared with that of external heat plates. Increasing the inlet flowrate helped to increase heat efficiency, but the heating efficiency would be limited if the flowrate exceeded 0.065 kg/s. The higher the liquid inlet temperature, the faster the heating. Nevertheless, if the inlet temperature was higher than 50 °C, the maximum temperature in battery pack may be above 40 °C. The inlet temperature of about 45 °C was appropriate to the system with

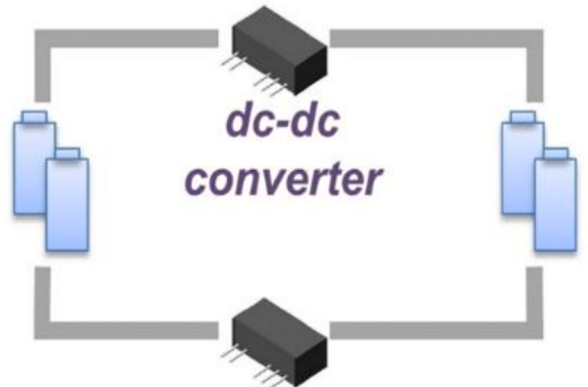


Fig. 19. Schematic diagram of mutual pulse heating [156].

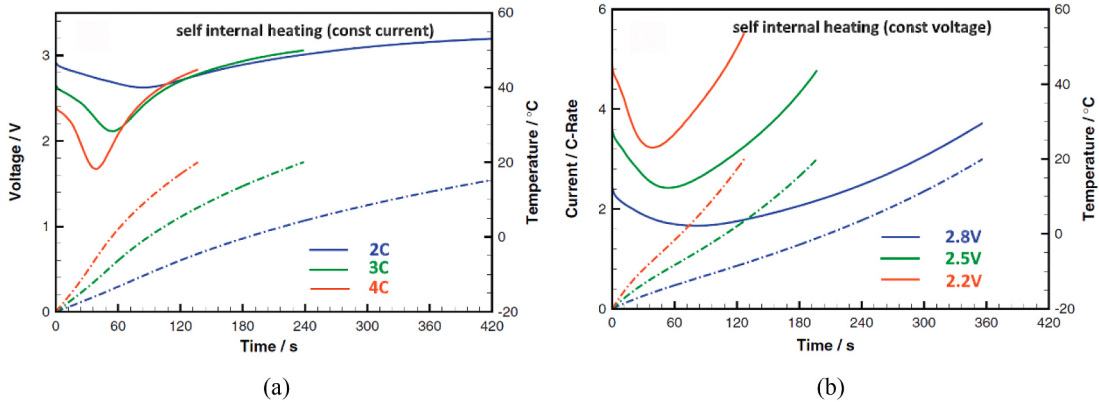
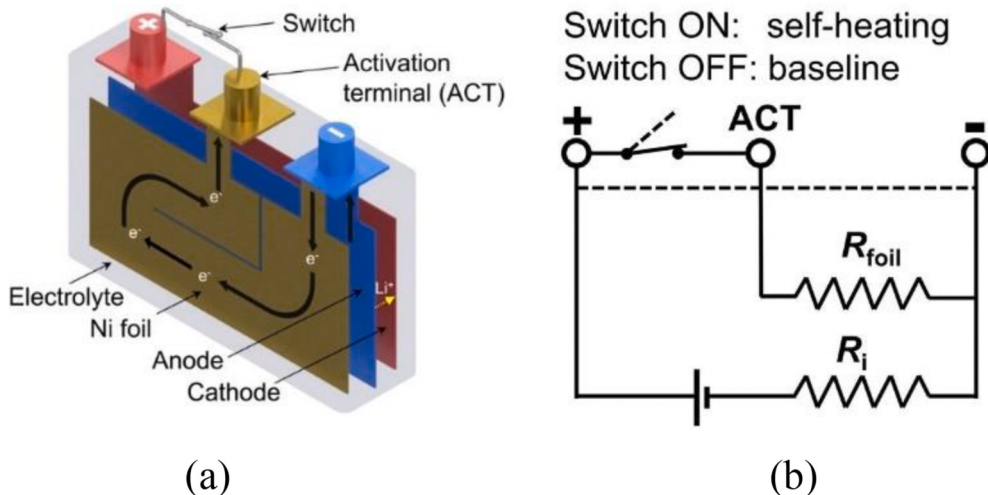
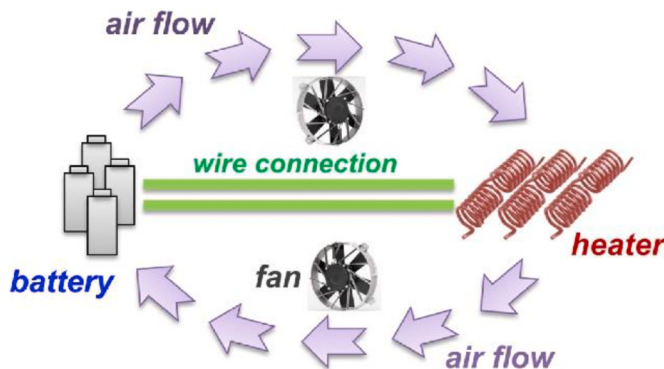


Fig. 18. Voltage, current and temperature variation curves of batteries in the process of internal resistance self-heating:(a) constant-current discharge; (b) constant-voltage discharge [156].



**Fig. 20.** Working principle of SHLB. (a) Schematic of SHLB structure. (b) Circuit diagram of self-heating [165].



**Fig. 21.** Schematic diagram of convection heating [156].

heat plates. For the liquid heating system, the heating loop can be incorporated into the liquid cooling loop and share parts with it, thereby reducing the weight and volume of the system, as shown in Fig. 22. Nelson [86] believed that silicone oil was a better heat-transfer medium than air. Adding insulation layer to the battery pack can effectively slow down the heating process after parking under high temperature and the cooling process after parking under low temperature. Wang et al. [173] designed simulated battery containers filled with atonal 324 to replace the battery. The feasibility of HP on heating cells at low temperature was verified by experiments. L-shaped HPs were inserted into the battery gap. HP can operate quickly after exposing at temperature of  $-15/-20^{\circ}\text{C}$  for more than 14 h, which proved that its performance was rarely

affected by low-temperature conditions. When the fluid temperature of HP evaporator was  $40^{\circ}\text{C}$ , the preheating time required for the simulated battery from  $-15 \pm 5^{\circ}\text{C}$  and  $-20 \pm 5^{\circ}\text{C}$  to  $0^{\circ}\text{C}$  was less than 300s and 500s respectively. When the fluid temperature was  $20^{\circ}\text{C}$ , the preheating time was less than 1200s and 1500s, respectively.

### 3.7.2. Heating with PCM

CPCMs have drawn extensive attention due to their high latent heat and compact structure without external power supply. Nevertheless, there are few researches focusing on the preheating and insulation of BTMS with CPCMs. A properly designed PCM-BTMS was beneficial for batteries at low temperature. Zhong et al. [174] developed a BTMS for 18,650 batteries based on CPCM coupled with resistance wire and fins. The coupled BTMS can not only prevent excessive temperature rise, but also achieve rapid preheating. The temperature at the center module increased by  $40^{\circ}\text{C}$  within 300s with the system. To maximize the function of fins, the battery module was designed as a strip to reduce the cells arranged along the width, as exhibited in Fig. 23. Fins enhanced the heat transfer efficiency to prevent thermal saturation of CPCM. The better the uniformity of temperature field, the smaller the voltage difference in the battery pack. PCMs positively contribute to the uniformity of the voltage and temperature fields. Ling et al. [175] prepared two kinds of CPCMs for 20-cells battery pack: 60 wt% RT44HC/fumed silica and 60 wt% RT44HC/EG. The BTMS based on the two CPCMs was compared respectively with the BTMS without PCM on thermal performance at  $5^{\circ}\text{C}$  and  $-10^{\circ}\text{C}$ . The results indicated that RT44HC/fumed silica composites had lower thermal conductivity, which led to larger temperature difference among cells, and the uneven temperature field resulted in voltage difference and capacity loss. Hence, RT44HC/fumed

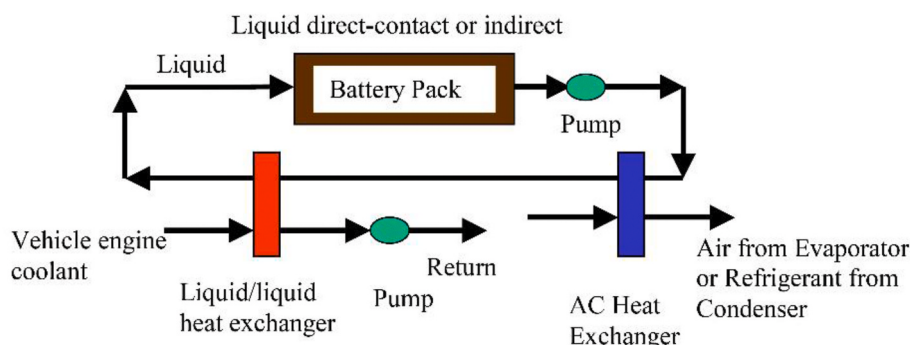


**Fig. 22.** Liquid cooling/heating cycle system [80].

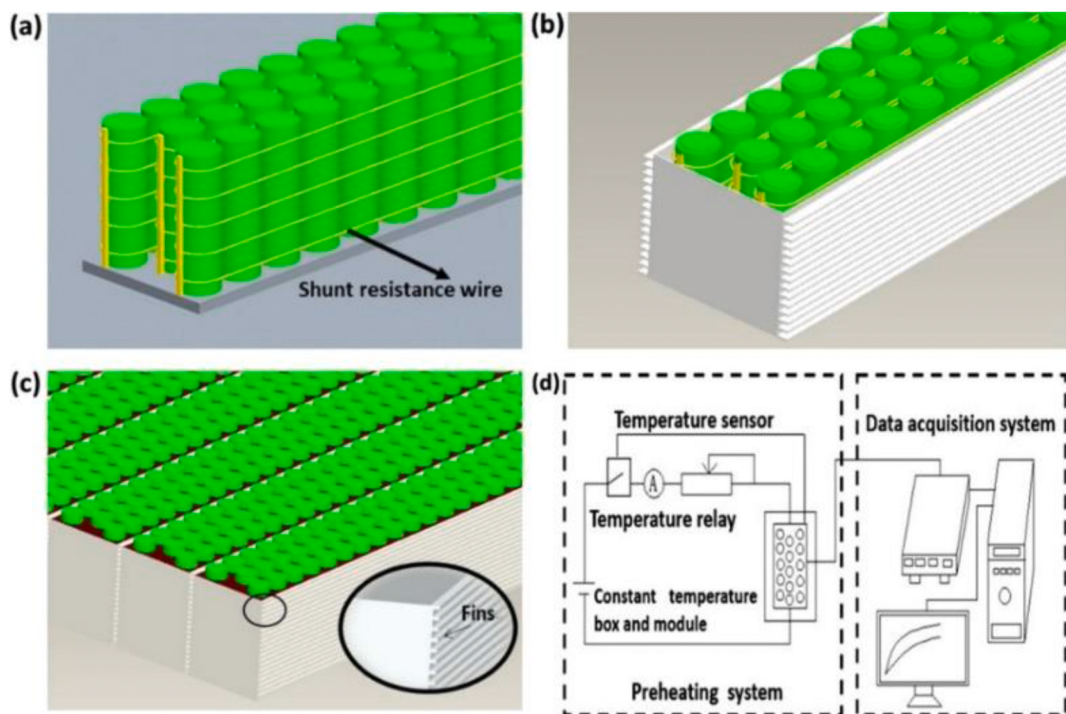


**Fig. 23.** Schematic diagram of BTMS: (a) The batteries wrapped with resistance wire. (b) Arrangement in battery module shell. (c) Arrangement in battery pack. (d) Preheating system [174].

silica CPCM wasn't suitable for the battery pack with multi cells. RT44HC/EG CPCM inhibited overheating and temperature fluctuation in the discharge test, and made the temperature and voltage distribution more uniform as the environmental temperature went from 5 °C to -10 °C. They argued that it was primary to make the temperature and voltage fields uniform, and RT44HC/EG CPCM had better thermal management performance at low temperature.

The active BTMS on the basis of automotive air-conditioning system was proposed in Ref. [176], and it was evaluated by the first law and second law of thermodynamics. The pentadecane ( $C_{15}H_{31}$ ) was chosen to be the heat-transfer medium for phase change slurry (PCS) cycle during preheating. It was proved that exergy efficiency of PCS cycle was higher than that of refrigerant cycle. Rao et al. [177] proposed 3D BTMS module based on PCMs. When the battery temperature was raised from 243.15 K to 283.15 K, the cold-start time required for air heating was 4.2 times longer than that for PCM. As the thermal conductivity of PCM had a fourfold rise, the temperature difference decreased by 5.3 °C. Huo et al. [178] established a lattice Boltzmann model for BTMS based on PCMs at low temperature, which considered the effects of latent heat, thermal conductivity and ambient temperature. Low thermal conductivity, high latent heat can slow down the solidification process of PCM, which had thermal insulation effect on the battery. They also demonstrated that increasing latent heat was the appropriate way to keep the battery warm at low temperature.

Table 7 compared and evaluated various battery heating methods from multiple perspectives. Each method has its advantages and disadvantages. In order to select the most appropriate heating strategy, the impact of the heating system on the battery capacity and the cycle life, as well as the manufacturing and maintenance costs, should be comprehensively evaluated based on the specification and operating conditions of the battery pack.

#### 4. Conclusion

EVs have drawn more and more attention, but its application and development are still affected by the performance and safety of lithium-

**Table 7**  
Comparison and evaluation of battery heating methods.

Criteria	Internal heating			External heating	
	DC heating	Pulse heating	SHLB	External heater	PCM
Initial cost	Low	Middle	Middle	High	Middle
Maintenance	Low	Middle	High	High	Middle
Major components	-	Circuit control module	Nickel foil, Switch	Electric heater, Fans	Resistance wire
Extra weight requirement	Light	Light	Light	Heavy	Heavy
Space	Low	Low	Low	High	Middle
Complexity	Simple	Complex	Complex	Complex	Middle
Effects on battery aging	Large	Middle	Middle	Little	Little
Risk of short circuit	Low	Low	High	Low	Low
Temperature gradient	Low	Low	Low	High	Middle
Heat loss	Small	Small	Small	Large	Large
Heating efficiency	Low	Middle	High	Middle	Middle
Battery cooling function	No	No	No	Yes	Yes

ion batteries. The lithium-ion battery has strict requirements on working temperature range. The electrochemical reaction inside battery is affected by temperature. The research progress of BTMS in recent years is reviewed from two aspects: cooling and preheating.

The cooling technologies of BTMS are summarized as follows based on cooling mediums:

- (1) Natural convection air-based BTMS is relatively simple in structure and low in production and maintenance cost. Forced convection air-cooling systems contain complex piping, fans, valve

- bodies, etc, which require additional energy to drive. These shortcomings may limit the application of forced air-cooling systems to EVs with higher performance and longer range. Optimizations of air flow channels and battery layout are the key research directions.
- (2) Compared with air cooling, liquid cooling system is better at keeping the battery temperature in the normal temperature range, and obtaining more uniform temperature distribution. However, the cooling performance gradually decreases along the direction of liquid flow. Liquid direct-cooling systems with mineral oil or silicon oil as coolant are appropriate for systems with high instantaneous heat generation. Liquid indirect-cooling system requires better leakproofness, and it's generally more complex and heavier than air-cooling system. Optimizations of channel shape and number design will be the main research directions. The properties of liquid metal as the coolant for battery packs still need further study.
  - (3) PCMs absorb the heat in the form of latent heat without consuming extra energy, thereby restraining the temperature rise of battery. The thermal conductivity of most PCMs is low, which directly affects the cooling efficiency. So, improving the thermal conductivity has been research hotspot of PCM. If the temperature rise is controlled only by PCMs in the continuous high-rate charging and discharging cycles, the thermal storage capacity may not be recovered timely, resulting in thermal runaway. Therefore, it's required to restore the energy storage capacity of PCMs through additional cooling module to assist in heat dissipation. The preparation of novel PCMs with high thermal conductivity, high latent heat and small volume expansion, as well as the active BTMS combined PCMs with forced heat-transfer module will become the key technologies on the research of PCM-BTMS.
  - (4) HP is more as a heat conduction tool and the heat still needs to be handled by active or passive means in most cases. Fins could be utilized to enlarge the heat-exchange area. To reduce the extra energy consumption and simplify the system structure, PCM/HP will be one of the trends of HP-based BTMS.

According to whether the heat source is the battery, the preheating technologies at low temperature is summarized as follows:

- (1) Internal resistance heating is the cheapest method, relying on ohmic heat to raise the battery temperature. It doesn't require additional components and avoids the heat loss from external heaters to the battery. AC heating is more efficient than DC heating. If reducing battery capacity decay is manufacturers' first priority, mutual pulse heating with dc-dc converters is preferred. Whereas, when the battery needs to be heated quickly, high charge/discharge rate is required. Attention should be paid to avoid the capacity attenuation caused by lithium precipitation.
- (2) SHLB inserts one or more pieces of nickel foil into the battery without the need for external heaters or electrolyte additives. The SHLB heating process has a lower temperature gradient and cost than the external heaters. Several pieces of nickel foil are more beneficial than a single nickel foil to decrease temperature gradient, shorten heating time and reduce energy consumption. The SHLB may cause a short circuit due to changes to the internal structure of the battery. Therefore, how to ensure safety is a critical issue.
- (3) For large battery cell and battery packs, external convection heating is not a good choice due to the long heat-conduction distance. Liquid heat plates and HP can preheat batteries and are feasible to share components with liquid-cooling and HP-cooling systems. Further researches should be carried out on liquid-loop design, liquid selection, HP layout and selection.

- (4) PCMs store heat with latent heat to keep the batteries warm for some time. Lower thermal conductivity can prolong the solidification period of PCM and the insulation time for batteries, but it will lead to larger temperature and voltage differences, as well as longer cold start-up time. After PCM is completely solidified, auxiliary preheating methods such as resistance wire and heating film are required. Therefore, the influence of thermal conductivity and latent heat on temperature uniformity, thermal insulation and preheating of battery pack should be considered comprehensively. The key of the research for PCM-based BTMS is to prolong the thermal-insulation time and shorten the preheating time without affecting the cooling performance.

The advantages and disadvantages of various BTMS are different, so it is critical to leverage the strengths of various systems. To sum up, the design of a novel BTMS integrating various methods will become the future research trend.

The battery pack is a key system in providing power for electric vehicles. In the future, the demand for high power, high energy density and high charging efficiency batteries will continue to grow, which will be followed by the demand for more efficient, more stable, more economical and more compact BTMS. From the perspective of low energy consumption and simplified structure, PCM based BTMS has potential, but further research is needed before it can be commercialized. First, it is necessary to enhance the thermal conductivity of PCM and reduce the cost when preparing novel PCMs. Second, in order to avoid the failure caused by the complete melting of PCM, it is necessary to explore the collaborative mechanism of various thermal management modes dominated by PCM, so as to ensure the durability of BTMS. Third, the research of preheating system is less than that of cooling system. An efficient, economical and safe battery rapid preheating system needs to be further developed. If the preheating and cooling systems can share components, it will be more in line with the development trend of lightweight and energy saving.

#### Declaration of competing interest

The authors declare that they have no known competing financial interests or personal relationships that could have appeared to influence the work reported in this paper.

#### Acknowledgements

This research was financially supported by the National Natural Science Foundation of China (51775393); Key R&D project of Hubei Province, China (2020BAB132); the 111 Project (B17034); Innovative Research Team Development Program of Ministry of Education of China (IRT\_17R83).

#### References

- [1] Feng X, Ouyang M, Liu X, Lu L, Xia Y, He X. Thermal runaway mechanism of lithium ion battery for electric vehicles: a review. *Energy Storage Mater* 2018;10: 246–67.
- [2] Wu T, Chen H, Wang Q, Sun J. Comparison analysis on the thermal runaway of lithium-ion battery under two heating modes. *J Hazard Mater* 2018;344:733–41.
- [3] Ren D, Feng X, Lu L, He X, Ouyang M. Overcharge behaviors and failure mechanism of lithium-ion batteries under different test conditions. *Appl Energy* 2019;250:323–32.
- [4] Li W, Xiao M, Peng X, Garg A, Gao L. A surrogate thermal modeling and parametric optimization of battery pack with air cooling for EVs. *Appl Therm Eng* 2019;147:90–100.
- [5] Kohlmeyer RR, Horrocks GA, Blake AJ, Yu ZN, Maruyama B, Huang H, et al. Pushing the thermal limits of Li-ion batteries. *Nanomater Energy* 2019;64: 103927.
- [6] Feng XN, Xu CS, He XM, Wang L, Zhang G, Ouyang MG. Mechanisms for the evolution of cell variations within a LiNi<sub>x</sub>CoyMn<sub>z</sub>O<sub>2</sub>/graphite lithium-ion battery pack caused by temperature non-uniformity. *J Clean Prod* 2018;205: 447–62.

- [7] Robinson JB, Darr JA, Eastwood DS, Hinds G, Lee PD, Shearing PR, et al. Non-uniform temperature distribution in Li-ion batteries during discharge - a combined thermal imaging, X-ray micro-tomography and electrochemical impedance approach. *J Power Sources* 2014;252:51–7.
- [8] Pesaran AA. Battery thermal models for hybrid vehicle simulations. *J Power Sources* 2002;110(2):377–82.
- [9] Huang YX, Lai HX. Effects of discharge rate on electrochemical and thermal characteristics of LiFePO<sub>4</sub>/graphite battery. *Appl Therm Eng* 2019;157:113744.
- [10] Chen MY, Ouyang DX, Liu JH, Wang J. Investigation on thermal and fire propagation behaviors of multiple lithium-ion batteries within the package. *Appl Therm Eng* 2019;157:113750.
- [11] Li QB, Yang CB, Santhanagopalan S, Smith K, Lamb J, Steele LA, et al. Numerical investigation of thermal runaway mitigation through a passive thermal management system. *J Power Sources* 2019;429:80–8.
- [12] Bandhauer TM, Garimella S, Fuller TF. A critical review of thermal issues in lithium-ion batteries. *J Electrochem Soc* 2011;158(3):R1–25.
- [13] Rao M, Zhang L, Li L, Rong L, Ye C, Zhou G, et al. Investigation of lithium content changes to understand the capacity fading mechanism in LiFePO<sub>4</sub>/graphite battery. *J Electroanal Chem* 2019;853:113544.
- [14] Nayak PK, Grinblat J, Levi E, Markovsky B, Aurbach D. Effect of cycling conditions on the electrochemical performance of high capacity Li and Mn-rich cathodes for Li<sup>+</sup>-ion batteries. *J Power Sources* 2016;318:9–17.
- [15] Li XK, Wang QQ, Yang YF, Kang JQ. Correlation between capacity loss and measurable parameters of lithium-ion batteries. *Int J Elec Power* 2019;110: 819–26.
- [16] Wang Q, Ping P, Zhao X, Chu G, Sun J, Chen C. Thermal runaway caused fire and explosion of lithium ion battery. *J Power Sources* 2012;208:210–24.
- [17] Hammami A, Raymond N, Armand M. Lithium-ion batteries: runaway risk of forming toxic compounds. *Nature* 2003;424(6949):635–6.
- [18] Wang Z, Yang H, Li Y, Wang G, Wang J. Thermal runaway and fire behaviors of large-scale lithium ion batteries with different heating methods. *J Hazard Mater* 2019;379:120730.
- [19] Chen MY, Ouyang DX, Weng JW, Liu JH, Wang J. Environmental pressure effects on thermal runaway and fire behaviors of lithium-ion battery with different cathodes and state of charge. *Process Saf Environ* 2019;130:250–6.
- [20] Wang Q, Mao B, Stolarov SI, Sun J. A review of lithium ion battery failure mechanisms and fire prevention strategies. *Prog Energ Combust* 2019;73:95–131.
- [21] Wilke S, Schweitzer B, Khateeb S, Al-Hallaj S. Preventing thermal runaway propagation in lithium ion battery packs using a phase change composite material: an experimental study. *J Power Sources* 2017;340:51–9.
- [22] Ji CW, Wang B, Wang SF, Pan S, Wang D, Qi PF, et al. Optimization on uniformity of lithium-ion cylindrical battery module by different arrangement strategy. *Appl Therm Eng* 2019;157.
- [23] Rao Z, Wang S. A review of power battery thermal energy management. *Renew Sustain Energy Rev* 2011;15(9):4554–71.
- [24] Siddique RM, Mahmud S, Heyst BV. A comprehensive review on a passive (phase change materials) and an active (thermoelectric cooler) battery thermal management system and their limitations. *J Power Sources* 2018;401:224–37.
- [25] Ali HM. Applications of combined/hybrid use of heat pipe and phase change materials in energy storage and cooling systems: a recent review. *J Energy Storage* 2019;26:100986.
- [26] Tauseef-ur-Rehman Ali HM, Janjua MM, Sajjad U, Yan WM. A critical review on heat transfer augmentation of phase change materials embedded with porous materials/foams. *Int J Heat Mass Tran* 2019;135:649–73.
- [27] Jaguemont J, Omar N, Van den Bossche P, Mierlo J. Phase-change materials (PCM) for automotive applications: a review. *Appl Therm Eng* 2018;132:308–20.
- [28] Regin AF, Solanki SC, Saini JS. Heat transfer characteristics of thermal energy storage system using PCM capsules: a review. *Renew Sustain Energy Rev* 2008;12(9):2438–58.
- [29] Zhao R, Zhang S, Liu J, Gu J. A review of thermal performance improving methods of lithium ion battery: electrode modification and thermal management system. *J Power Sources* 2015;299:557–77.
- [30] Madani SS, Swierczynski MZ, Kaer SK. A review of thermal management and safety for lithium ion batteries. In: 12th international conference on ecological vehicles and renewable energies (EVER); 2017. Monaco.
- [31] Bernardi D, Pawlikowski E, Newman J. A general energy balance for battery systems. *J Electrochem Soc* 1985;132(1):5–12.
- [32] Xie Y, Shi S, Tang J, Wu H, Yu J. Experimental and analytical study on heat generation characteristics of a lithium-ion power battery. *Int J Heat Mass Tran* 2018;122:884–94.
- [33] Lin X, Perez HE, Mohan S, Siegel JB, Stefanopoulou AG, Ding Y, et al. A lumped-parameter electro-thermal model for cylindrical batteries. *J Power Sources* 2014; 257:1–11.
- [34] Alifai W, Zhang C, Uddin K, Worwood D, Dinh TQ, Ormeno PA, et al. A lumped thermal model of lithium-ion battery cells considering radiative heat transfer. *Appl Therm Eng* 2018;143:472–81.
- [35] Xie Y, Li W, Hu XS, Lin XK, Zhang YJ, Dan D, et al. An enhanced online temperature estimation for lithium-ion batteries. *IEEE T Transp Electr* 2020;6(2): 375–90.
- [36] Richardson RR, Howey DA. Sensorless battery internal temperature estimation using a kalman filter with impedance measurement. *IEEE T Sustain Energ* 2015; 4(4):1190–9.
- [37] Tao W, Tseng KJ, Shan Y, Hu X. Development of a one-dimensional thermal-electrochemical model of lithium ion battery. In: 39th annual conference of the IEEE industrial-electronics-society (IECON). Vienna, Austria; Year, p. 6709–6714.
- [38] L. Lee J, Chemistruck A, L.Plett G. One-dimensional physics-based reduced-order model of lithium-ion dynamics. *J Power Sources* 2012;220:430–48.
- [39] Tourani A, White P, Ivey P. A multi scale multi-dimensional thermo electrochemical modelling of high capacity lithium-ion cells. *J Power Sources* 2014;255:360–7.
- [40] Xu M, Zhang Z, Wang X, Jia L, Yang L. Two-dimensional electrochemical-thermal coupled modeling of cylindrical LiFePO<sub>4</sub> batteries. *J Power Sources* 2014;256: 233–43.
- [41] An Z, Jia L, Wei L, Yang C. Numerical modeling and analysis of thermal behavior and Li<sup>+</sup> transport characteristic in lithium-ion battery. *Int J Heat Mass Tran* 2018;127:1351–66.
- [42] Ghalkhani M, Bahiraei F, Nazri G-A, Saif M. Electrochemical-thermal model of pouch-type lithium-ion batteries. *Electrochim Acta* 2017;247:569–87.
- [43] McCleary DAH, Meyers JP, Kim B. Three-dimensional modeling of electrochemical performance and heat generation of spirally and prismatically wound lithium-ion batteries. *J Electrochem Soc* 2013;160(11):A1931–43.
- [44] Xie Y, He XJ, Li W, Zhang YJ, Dan D, Lee KN, et al. A novel electro-thermal coupled model of lithium-ion pouch battery covering heat generation distribution and tab thermal behaviours. *Int J Energy Res* 2020;44(14):11725–41.
- [45] Feng X, He X, Ouyang M, Wang L, Lu L, Ren D, et al. A coupled electrochemical-thermal failure model for predicting the thermal runaway behavior of lithium-ion batteries. *J Electrochem Soc* 2018;165(16):A3748–65.
- [46] Ren D, Feng X, Lu L, Ouyang M, Zheng S, Li J, et al. An electrochemical-thermal coupled overcharge-to-thermal-runaway model for lithium ion battery. *J Power Sources* 2017;364:328–40.
- [47] Teng H, Yeow K. Design of direct and indirect liquid cooling systems for high-capacity, high-power lithium-ion battery packs. *SAE Int J Alt Power* 2012;1(2): 525–36.
- [48] Cho GY, Choi JW, Park JH, Cha SW. Transient modeling and validation of lithium ion battery pack with air cooled thermal management system for electric vehicles. *Int J Auto Tech-Kor* 2014;15(5):795–803.
- [49] Choi YS, Kang DM. Prediction of thermal behaviors of an air-cooled lithium-ion battery system for hybrid electric vehicles. *J Power Sources* 2014;270:273–80.
- [50] Wang T, Tseng KJ, Zhao J. Development of efficient air-cooling strategies for lithium-ion battery module based on empirical heat source model. *Appl Therm Eng* 2015;90:521–9.
- [51] Yu X, Lu Z, Zhang L, Wei L, Cui X, Jin L. Experimental study on transient thermal characteristics of stagger-arranged lithium-ion battery pack with air cooling strategy. *Int J Heat Mass Tran* 2019;143:118576.
- [52] Zolot Matthew, Pesaran Ahmad A, Mihalic Mark. Thermal evaluation of Toyota Prius battery pack. Future Car Congress 2002. <https://doi.org/10.4271/2002-01-1962>.
- [53] Wei Z, Zhao J, Xiong B. Dynamic electro-thermal modeling of all-vanadium redox flow battery with forced cooling strategies. *Appl Energy* 2014;135:1–10.
- [54] Pesaran Ahmad, Vlahinos Andreas, Stuart Thomas. Cooling and preheating of batteries in hybrid electric vehicles. In: The 6th ASME-JSME Thermal Engineering Joint Conference. Hawaii Island: JSME; 2003. p. 1–7.
- [55] Lu Z, Yu XL, Wei LC, Qiu YL, Zhang LY, Meng XZ, et al. Parametric study of forced air cooling strategy for lithium-ion battery pack with staggered arrangement. *Appl Therm Eng* 2018;136:28–40.
- [56] Lu Z, Meng XZ, Wei LC, Hu WY, Zhang LY, Jin LW. Thermal management of densely-packed EV battery with forced air cooling strategies. *Energy Procedia* 2016;88:682–8.
- [57] Lemmon EW, Jacobsen RT. Viscosity and Thermal Conductivity Equations for nitrogen, oxygen, argon, and air. *Int J Thermophys* 2004;25(1):21–69.
- [58] Malik M, Dincer I, Rosen MA, Mathew M, Fowler M. Thermal and electrical performance evaluations of series connected Li-ion batteries in a pack with liquid cooling. *Appl Therm Eng* 2018;129:472–81.
- [59] Al-Zareer M, Dincer I, Rosen MA. A novel approach for performance improvement of liquid to vapor based battery cooling systems. *Energy Convers Manag* 2019; 187:191–204.
- [60] Xu X, Li W, Xu B, Qin J. Numerical study on a water cooling system for prismatic LiFePO<sub>4</sub> batteries at abused operating conditions. *Appl Energy* 2019;250:404–12.
- [61] Liu H, Wei Z, He W, Zhao J. Thermal issues about Li-ion batteries and recent progress in battery thermal management systems: a review. *Energy Convers Manag* 2017;150:304–30.
- [62] Yang N, Zhang X, Li G, Hua D. Assessment of the forced air-cooling performance for cylindrical lithium-ion battery packs: a comparative analysis between aligned and staggered cell arrangements. *Appl Therm Eng* 2015;80:55–65.
- [63] Yu K, Yang X, Cheng Y, Li C. Thermal analysis and two-directional air flow thermal management for lithium-ion battery pack. *J Power Sources* 2014;270: 193–200.
- [64] Tong W, Somasundaram K, Birgersson E, Mujumdar AS, Yap C. Thermo-electrochemical model for forced convection air cooling of a lithium-ion battery module. *Appl Therm Eng* 2016;99:672–82.
- [65] Fan Y, Bao Y, Ling C, Chu Y, Tan X, Yang S. Experimental study on the thermal management performance of air cooling for high energy density cylindrical lithium-ion batteries. *Appl Therm Eng* 2019;155:96–109.
- [66] E J, Yue M, Chen J, Zhu H, Deng Y, Zhu Y, et al. Effects of the different air cooling strategies on cooling performance of a lithium-ion battery module with baffle. *Appl Therm Eng* 2018;144:231–41.
- [67] Xu XM, He R. Research on the heat dissipation performance of battery pack based on forced air cooling. *J Power Sources* 2013;240:33–41.
- [68] Park H. A design of air flow configuration for cooling lithium ion battery in hybrid electric vehicles. *J Power Sources* 2013;239:30–6.

- [69] Sun H, Dixon R. Development of cooling strategy for an air cooled lithium-ion battery pack. *J Power Sources* 2014;272:404–14.
- [70] Chen K, Li Z, Chen Y, Long S, Hou J, Song M, et al. Design of parallel air-cooled battery thermal management system through numerical study. *Energies* 2017;10(10).
- [71] Chen K, Chen Y, Li Z, Yuan F, Wang S. Design of the cell spacings of battery pack in parallel air-cooled battery thermal management system. *Int J Heat Mass Tran* 2018;127:393–401.
- [72] Chen K, Wang SF, Song MX, Chen L. Configuration optimization of battery pack in parallel air-cooled battery thermal management system using an optimization strategy. *Appl Therm Eng* 2017;123:177–86.
- [73] Chen K, Wang S, Song M, Chen L. Structure optimization of parallel air-cooled battery thermal management system. *Int J Heat Mass Tran* 2017;111:943–52.
- [74] Chen K, Song M, Wei W, Wang S. Structure optimization of parallel air-cooled battery thermal management system with U-type flow for cooling efficiency improvement. *Energy* 2018;145:603–13.
- [75] Chen K, Wu W, Yuan F, Chen L, Wang S. Cooling efficiency improvement of air-cooled battery thermal management system through designing the flow pattern. *Energy* 2019;167:781–90.
- [76] Xie J, Ge Z, Zang M, Wang S. Structural optimization of lithium-ion battery pack with forced air cooling system. *Appl Therm Eng* 2017;126:583–93.
- [77] Hong S, Zhang X, Chen K, Wang S. Design of flow configuration for parallel air-cooled battery thermal management system with secondary vent. *Int J Heat Mass Tran* 2018;116:1204–12.
- [78] Fan L, Khodadadi JM, Pesaran AA. A parametric study on thermal management of an air-cooled lithium-ion battery module for plug-in hybrid electric vehicles. *J Power Sources* 2013;238:301–12.
- [79] Park S, Jung D. Battery cell arrangement and heat transfer fluid effects on the parasitic power consumption and the cell temperature distribution in a hybrid electric vehicle. *J Power Sources* 2013;227:191–8.
- [80] Pesaran AA. Battery thermal management in EVs and HEVs: issues and solutions. In: Advanced automotive battery conference; 2001. Las Vegas, USA.
- [81] Hirano H, Tajima T, Hasegawa T, Sekiguchi T, Uchino M. Boiling liquid battery cooling for electric vehicle. In: IEEE conference and expo transportation electrification asia-pacific (ITEC asia-pacific); 2014. Beijing, China.
- [82] van Gils RW, Danilov D, Notten PHL, Speetjens MPM, Nijmeijer H. Battery thermal management by boiling heat-transfer. *Energy Convers Manag* 2014;79:9–17.
- [83] R. Pendegast D, P.DeMauro E, Fletcher M, Stimson E, C.Mollendorf J. A rechargeable lithium-ion battery module for underwater use. *J Power Sources* 2011;196(2):793–800.
- [84] Kim GH, Pesaran Ahmad A. Battery thermal management system design modeling. In: the 22nd international battery, hybrid and fuel cell electric vehicle conference and exhibition; 2006. p. 1–16. Yokohama, Japan.
- [85] Karimi G, Li X. Thermal management of lithium-ion batteries for electric vehicles. *Int J Energy Res* 2013;37(1):13–24.
- [86] Nelson P, Dees D, Amine K, Henriksen G. Modeling thermal management of lithium-ion PNGV batteries. *J Power Sources* 2002;110:349–56.
- [87] Luo Y, Luo B, Lang C. A research on the direct contact liquid cooling method of Lithium-ion battery pack. *Automot Eng* 2016;38(7):909–14 [in Chinese].
- [88] Karimi G, Dehghan AR. Thermal analysis of high-power lithium-ion battery packs using flow network approach. *Int J Energy Res* 2014;38(14):1793–811.
- [89] Chen D, Jiang J, Kim G-H, Yang C, Pesaran A. Comparison of different cooling methods for lithium ion battery cells. *Appl Therm Eng* 2016;94:846–54.
- [90] Chacko S, Charmer S. Lithium-ion pack thermal modeling and evaluation of indirect liquid cooling for electric vehicle battery thermal management. In: innovations in Fuel Economy and Sustainable Road Transport Conference. Pune, India 2011;13–21.
- [91] Krüger I, Schmitz G. Energy consumption of battery cooling in hybrid electric vehicles. In: International refrigeration and air conditioning conference; 2012. West Lafayette, America.
- [92] Panchal S, Dincer I, Agelin-Chaab M, Fraser R, Fowler M. Thermal modeling and validation of temperature distributions in a prismatic lithium-ion battery at different discharge rates and varying boundary conditions. *Appl Therm Eng* 2016;96:190–9.
- [93] Wang C, Zhang G, Li X, Huang J, Wang Z, Lv Y, et al. Experimental examination of large capacity LiFePO<sub>4</sub> battery pack at high temperature and rapid discharge using novel liquid cooling strategy. *Int J Energy Res* 2018;42(3):1172–82.
- [94] Yang X, Tan S, Liu J. Thermal management of Li-ion battery with liquid metal. *Energy Convers Manag* 2016;117:577–85.
- [95] Deng Y, Liu J. A liquid metal cooling system for the thermal management of high power LEDs. *Int Commun Heat Mass* 2010;37(7):788–91.
- [96] Li T, Lv Y-G, Liu J, Zhou Y-X. A powerful way of cooling computer chip using liquid metal with low melting point as the cooling fluid. *Forsch Ingenieurwes* 2006;70(4):243–51.
- [97] Lorenzin N, Abánades A. A review on the application of liquid metals as heat transfer fluid in Concentrated Solar Power technologies. *Int J Hydrogen Energy* 2016;41(17):6990–5.
- [98] Chung Y, Kim MS. Thermal analysis and pack level design of battery thermal management system with liquid cooling for electric vehicles. *Energy Convers Manag* 2019;196:105–16.
- [99] Jin LW, Lee PS, Kong XX, Fan Y, Chou SK. Ultra-thin minichannel LCP for EV battery thermal management. *Appl Energy* 2014;113:1786–94.
- [100] Zhao J, Rao Z, Li Y. Thermal performance of mini-channel liquid cooled cylinder based battery thermal management for cylindrical lithium-ion power battery. *Energy Convers Manag* 2015;103:157–65.
- [101] Qian Z, Li Y, Rao Z. Thermal performance of lithium-ion battery thermal management system by using mini-channel cooling. *Energy Convers Manag* 2016;126:622–31.
- [102] Jarrett A, Kim IY. Design optimization of electric vehicle battery cooling plates for thermal performance. *J Power Sources* 2011;196(23):10359–68.
- [103] Zhao C, Sousa ACM, Jiang F. Minimization of thermal non-uniformity in lithium-ion battery pack cooled by channelized liquid flow. *Int J Heat Mass Tran* 2019;129:660–70.
- [104] Deng T, Zhang G, Ran Y. Study on thermal management of rectangular Li-ion battery with serpentine-channel cold plate. *Int J Heat Mass Tran* 2018;125:143–52.
- [105] Rao Z, Qian Z, Kuang Y, Li Y. Thermal performance of liquid cooling based thermal management system for cylindrical lithium-ion battery module with variable contact surface. *Appl Therm Eng* 2017;123:1514–22.
- [106] Liu H, Chika E, Zhao J. Investigation into the effectiveness of nanofluids on the mini-channel thermal management for high power lithium ion battery. *Appl Therm Eng* 2018;142:511–23.
- [107] Zalba B, Marín JM, Cabeza LF, Mehling H. Review on thermal energy storage with phase change: materials, heat transfer analysis and applications. *Appl Therm Eng* 2003;23:251–83.
- [108] Liu Z, Sun X, Ma C. Experimental investigations on the characteristics of melting processes of stearic acid in an annulus and its thermal conductivity enhancement by fins. *Energy Convers Manag* 2005;46(6):959–69.
- [109] Ping P, Peng R, Kong D, Chen G, Wen J. Investigation on thermal management performance of PCM-fin structure for Li-ion battery module in high-temperature environment. *Energy Convers Manag* 2018;176:131–46.
- [110] Sabbah R, Kizilel R, Selman JR, Al-Hallaj S. Active (air-cooled) vs. passive (phase change material) thermal management of high power lithium-ion packs: limitation of temperature rise and uniformity of temperature distribution. *J Power Sources* 2008;182(2):630–8.
- [111] Lazrak A, Fourmigue J-F, Robin J-F. An innovative practical battery thermal management system based on phase change materials: numerical and experimental investigations. *Appl Therm Eng* 2018;128:20–32.
- [112] Kizilel R, Sabbah R, Selman JR, Al-Hallaj S. An alternative cooling system to enhance the safety of Li-ion battery packs. *J Power Sources* 2009;194(2):1105–12.
- [113] Wang Z, Zhang Z, Jia L, Yang L. Paraffin and paraffin/aluminum foam composite phase change material heat storage experimental study based on thermal management of Li-ion battery. *Appl Therm Eng* 2015;78:428–36.
- [114] Zhang Z, Zhang N, Peng J, Fang X, Gao X, Fang Y. Preparation and thermal energy storage properties of paraffin/expanded graphite composite phase change material. *Appl Energy* 2012;91(1):426–31.
- [115] Jiang G, Huang J, Fu Y, Cao M, Liu M. Thermal optimization of composite phase change material/expanded graphite for Li-ion battery thermal management. *Appl Therm Eng* 2016;108:1119–25.
- [116] Rao Z, Huo Y, Liu X, Zhang G. Experimental investigation of battery thermal management system for electric vehicle based on paraffin/copper foam. *J Energy Inst* 2015;88(3):241–6.
- [117] Wu W, Yang X, Zhang G, Ke X, Wang Z, Situ W, et al. An experimental study of thermal management system using copper mesh-enhanced composite phase change materials for power battery pack. *Energy* 2016;113:909–16.
- [118] Lv Y, Yang X, Li X, Zhang G, Wang Z, Yang C. Experimental study on a novel battery thermal management technology based on low density polyethylene-enhanced composite phase change materials coupled with low fins. *Appl Energy* 2016;178:376–82.
- [119] He J, Yang X, Zhang G. A phase change material with enhanced thermal conductivity and secondary heat dissipation capability by introducing a binary thermal conductive skeleton for battery thermal management. *Appl Therm Eng* 2019;148:984–91.
- [120] Zhang X, Liu C, Rao Z. Experimental investigation on thermal management performance of electric vehicle power battery using composite phase change material. *J Clean Prod* 2018;201:916–24.
- [121] Hussain A, Tso CY, Chao CYH. Experimental investigation of a passive thermal management system for high-powered lithium ion batteries using nickel foam-paraffin composite. *Energy* 2016;115:209–18.
- [122] Azizi Y, Sadrameli SM. Thermal management of a LiFePO<sub>4</sub> battery pack at high temperature environment using a composite of phase change materials and aluminum wire mesh plates. *Energy Convers Manag* 2016;128:294–302.
- [123] Chen Z, Gao D, Shi J. Experimental and numerical study on melting of phase change materials in metal foams at pore scale. *Int J Heat Mass Tran* 2014;72:646–55.
- [124] Zou D, Liu X, He R, Zhu S, Bao J, Guo J, et al. Preparation of a novel composite phase change material (PCM) and its locally enhanced heat transfer for power battery module. *Energy Convers Manag* 2019;180:1196–202.
- [125] Goli P, Legedza S, Dhar A, Salgado R, Renteria J, Balandin AA. Graphene-enhanced hybrid phase change materials for thermal management of Li-ion batteries. *J Power Sources* 2014;248:37–43.
- [126] Chan KC, Tso CY, Hussain A, Chao CYH. A theoretical model for the effective thermal conductivity of graphene coated metal foams. *Appl Therm Eng* 2019;161.
- [127] Hussain A, Abidi IH, Tso CY, Chan KC, Luo Z, Chao CYH. Thermal management of lithium ion batteries using graphene coated nickel foam saturated with phase change materials. *Int J Therm Sci* 2018;124:23–35.
- [128] Wu W, Wu W, Wang S. Thermal management optimization of a prismatic battery with shape-stabilized phase change material. *Int J Heat Mass Tran* 2018;121:967–77.

- [129] Zhang G, Rao Z, Wu Z. Experimental investigation on the heat dissipation effect of power battery pack cooled with phase change materials. *Chem Ind Eng Prog* 2009;28(1):23–6 [in Chinese].
- [130] Kizilel R, Lateef A, Sabbah R, Farid MM, Selman JR, Al-Hallaj S. Passive control of temperature excursion and uniformity in high-energy Li-ion battery packs at high current and ambient temperature. *J Power Sources* 2008;183(1):370–5.
- [131] Schweitzer B, Wilke S, Khateeb S, Al-Hallaj S. Experimental validation of a 0-D numerical model for phase change thermal management systems in lithium-ion batteries. *J Power Sources* 2015;287:211–9.
- [132] Lin C, Xu S, Chang G, Liu J. Experiment and simulation of a LiFePO<sub>4</sub> battery pack with a passive thermal management system using composite phase change material and graphite sheets. *J Power Sources* 2015;275:742–9.
- [133] Alipanah M, Li X. Numerical studies of lithium-ion battery thermal management systems using phase change materials and metal foams. *Int J Heat Mass Tran* 2016;102:1159–68.
- [134] Wang C, Lin T, Li N, Zheng H. Heat transfer enhancement of phase change composite material: copper foam/paraffin. *Renew Energy* 2016;96:960–5.
- [135] Fathabadi H. High thermal performance lithium-ion battery pack including hybrid active-passive thermal management system for using in hybrid/electric vehicles. *Energy* 2014;70:529–38.
- [136] Ling Z, Wang F, Fang X, Gao X, Zhang Z. A hybrid thermal management system for lithium ion batteries combining phase change materials with forced-air cooling. *Appl Energy* 2015;148:403–9.
- [137] Weng J, Ouyang D, Yang X, Chen M, Zhang G, Wang J. Optimization of the internal fin in a phase-change-material module for battery thermal management. *Appl Therm Eng* 2019;114698.
- [138] Srimuang W, Amatachaya P. A review of the applications of heat pipe heat exchangers for heat recovery. *Renew Sustain Energy Rev* 2012;16(6):4303–15.
- [139] Narcy M, Lips S, Sartre V. Experimental investigation of a confined flat two-phase thermosyphon for electronics cooling. *Exp Therm Fluid Sci* 2018;96:516–29.
- [140] Kim J, Oh J, Lee H. Review on battery thermal management system for electric vehicles. *Appl Therm Eng* 2019;149:192–212.
- [141] Feng L, Zhou S, Li Y, Wang Y, Zhao Q, Luo C, et al. Experimental investigation of thermal and strain management for lithium-ion battery pack in heat pipe cooling. *J Energy Storage* 2018;16:84–92.
- [142] Liang J, Gan Y, Li Y. Investigation on the thermal performance of a battery thermal management system using heat pipe under different ambient temperatures. *Energy Convers Manag* 2018;155:1–9.
- [143] Zhao J, Lv P, Rao Z. Experimental study on the thermal management performance of phase change material coupled with heat pipe for cylindrical power battery pack. *Exp Therm Fluid Sci* 2017;82:182–8.
- [144] Wu W, Yang X, Zhang G, Chen K, Wang S. Experimental investigation on the thermal performance of heat pipe-assisted phase change material based battery thermal management system. *Energy Convers Manag* 2017;138:486–92.
- [145] Wang Q, Rao Z, Huo Y, Wang S. Thermal performance of phase change material/oscillating heat pipe-based battery thermal management system. *Int J Therm Sci* 2016;102:9–16.
- [146] Zhuang B, Deng W, Tang Y, Ding X, Chen K, Zhong G, et al. Experimental investigation on a novel composite heat pipe with phase change materials coated on the adiabatic section. *Int Commun Heat Mass* 2019;100:42–50.
- [147] Liu F, Lan F, Chen J. Dynamic thermal characteristics of heat pipe via segmented thermal resistance model for electric vehicle battery cooling. *J Power Sources* 2016;321:57–70.
- [148] Huang CK, Sakamoto JS, Wolfenstine J, Surampudi S. The limits of low-temperature performance of Li-ion cells. *J Electrochem Soc* 2000;147(8):2893–6.
- [149] Yi J, Kim U, Shin C, Han T, Park S. Modeling the temperature dependence of the discharge behavior of a lithium-ion battery in low environmental temperature. *J Power Sources* 2013;244:143–8.
- [150] Ji Y, Zhang Y, Wang C. Li-ion cell operation at low temperatures. *J Electrochem Soc* 2013;160(4):A636–49.
- [151] Wang F, Chen J, Tan Z, Wu M, Yi B, Su W, et al. Low-temperature electrochemical performances of LiFePO<sub>4</sub> cathode materials for lithium ion batteries. *J Taiwan Inst Chem E* 2014;45(4):1321–30.
- [152] Park G, Gunawardhana N, Nakamura H, Lee Y, Yoshio M. The study of electrochemical properties and lithium deposition of graphite at low temperature. *J Power Sources* 2012;199:293–9.
- [153] Foss CEL, Svensson AM, Gullbrekken O, Sunde S, Vullum-Bruer F. Temperature effects on performance of graphite anodes in carbonate based electrolytes for lithium ion batteries. *Journal of Energy Storage* 2018;17:395–402.
- [154] Senyshyn A, Muhlbauer MJ, Dolotko O, Ehrenberg H. Low-temperature performance of Li-ion batteries: the behavior of lithiated graphite. *J Power Sources* 2015;282:235–40.
- [155] Lu Z, Yu XL, Wei LC, Cao F, Zhang LY, Meng XZ, et al. A comprehensive experimental study on temperature-dependent performance of lithium-ion battery. *Appl Therm Eng* 2019;158.
- [156] Ji Y, Wang CY. Heating strategies for Li-ion batteries operated from subzero temperatures. *Electrochim Acta* 2013;107:664–74.
- [157] Petzl M, Kasper M, Danzer MA. Lithium plating in a commercial lithium-ion battery A low-temperature aging study. *J Power Sources* 2015;275:799–807.
- [158] Wu C, Chang C, Avdeev M, Pan P-I, Li W. In operando detection of lithium diffusion behaviors at low temperature in 18650 Li-ion battery anode. *Physica B* 2018;551:305–8.
- [159] Qu Z, Jiang Z, Wang Q. Experimental study on pulse self-heating of lithium-ion battery at low temperature. *Int J Heat Mass Tran* 2019;135:696–705.
- [160] Zhu J, Sun Z, Wei X, Dai H, Gu W. Experimental investigations of an AC pulse heating method for vehicular high power lithium-ion batteries at subzero temperatures. *J Power Sources* 2017;367:145–57.
- [161] Zhang J, Ge H, Li Z, Ding Z. Internal heating of lithium-ion batteries using alternating current based on the heat generation model in frequency domain. *J Power Sources* 2015;273:1030–7.
- [162] Zhao X, Zhang G, Yang L, Qiang J, Chen Z. A new charging mode of Li-ion batteries with LiFePO<sub>4</sub>/C composites under low temperature. *J Therm Anal Calorim* 2011;104(2):561–7.
- [163] Ruan H, Jiang J, Sun B, Zhang W, Gao W, Wang LY, et al. A rapid low-temperature internal heating strategy with optimal frequency based on constant polarization voltage for lithium-ion batteries. *Appl Energy* 2016;177:771–82.
- [164] Wang CY, Zhang G, Ge S, Xu T, Ji Y, Yang XG, et al. Lithium-ion battery structure that self-heats at low temperatures. *Nature* 2016;529(7587):515–8.
- [165] Zhang G, Ge S, Xu T, Yang X-G, Tian H, Wang C-Y. Rapid self-heating and internal temperature sensing of lithium-ion batteries at low temperatures. *Electrochim Acta* 2016;218:149–55.
- [166] Yang X, Zhang G, Wang C. Computational design and refinement of self-heating lithium ion batteries. *J Power Sources* 2016;328:203–11.
- [167] Yang X, Liu T, Wang C. Innovative heating of large-size automotive Li-ion cells. *J Power Sources* 2017;342:598–604.
- [168] Lei Z, Zhang Y, Lei X. Improving temperature uniformity of a lithium-ion battery by intermittent heating method in cold climate. *Int J Heat Mass Tran* 2018;121:275–81.
- [169] Lei Z, Zhang Y, Lei X. Temperature uniformity of a heated lithium-ion battery cell in cold climate. *Appl Therm Eng* 2018;129:148–54.
- [170] Li J, Wu P, Tian H. Researches on heating low-temperature lithium-ion power battery in electric vehicles. In: Transportation electrification asia-pacific; 2014. p. 1–6. Beijing, China.
- [171] Song H, Jeong J, Lee B, Shin D, Kim B, Kim T, et al. Experimental study on the effects of pre-heating a battery in a low-temperature environment. In: 2012 IEEE vehicle power and propulsion conference; 2012. p. 1198–201. Seoul, Korea.
- [172] Fan R, Zhang C, Wang Y, Ji C, Meng Z, Xu L, et al. Numerical study on the effects of battery heating in cold climate. *J Energy Storage* 2019;26.
- [173] Wang Q, Jiang B, Xue QF, Sun HL, Li B, Zou HM, et al. Experimental investigation on EV battery cooling and heating by heat pipes. *Appl Therm Eng* 2015;88:54–60.
- [174] Zhong G, Zhang G, Yang X, Li X, Wang Z, Yang C, et al. Researches of composite phase change material/cooling/resistance wire preheating coupling system of a designed 18650-type battery module. *Appl Therm Eng* 2017;127:176–83.
- [175] Ling Z, Wen X, Zhang Z, Fang X, Gao X. Thermal management performance of phase change materials with different thermal conductivities for Li-ion battery packs operated at low temperatures. *Energy* 2018;144:977–83.
- [176] Zhang X, Kong X, Li G, Li J. Thermodynamic assessment of active cooling/heating methods for lithium-ion batteries of electric vehicles in extreme conditions. *Energy* 2014;64:1092–101.
- [177] Rao ZH, Wang SF, Zhang YL. Thermal management with phase change material for a power battery under cold temperatures. *Energy Sources Part A* 2014;36(20):2287–95.
- [178] Huo Y, Rao Z. Investigation of phase change material based battery thermal management at cold temperature using lattice Boltzmann method. *Energy Convers Manag* 2017;133:204–15.